博士論文

Herpes Simplex Virus 1 Protein UL47 and Host Cell Protein p32 Interact in Infected Cells to Regulate Viral Nuclear Egress

（HSV-1 主要構成因子 UL47 は宿主細胞因子 p32 と相互作用し、ウイルスの核出芽を制御する）

刘 卓明

Context

Abstract

Herpesviruses have evolved a unique mechanism for nuclear egress of nascent progeny nuclocapsids: the nucleocapsids bud through the inner nuclear membrane into the perinuclear space between the inner and outer nuclear membranes (primary envelopment) and enveloped nucleocapsids then fuse with the outer nuclear membrane to release nucleocapsids into the cytoplasm (de-envelopment). We have shown that the herpes simplex virus 1 (HSV-1) encorded major virion structural protein UL47 and cellular protein p32, that UL47 binds, are novel regulators for HSV-1 nuclear egress. In particular: (i) p32 was redistributed from the cytoplasm to the nuclear membrane in HSV-1-infected cells and UL47 was required for this redistribution; (ii) UL47 formed a complex(es) with p32 and also with HSV-1 proteins UL34, UL31, and/or Us3, which have all been reported to be critical for viral nuclear egress, and these viral proteins and p32 co-localized at the nuclear membrane in HSV-1-infected cells; (iii) the UL47-null mutation considerably reduced primary enveloped virions in the perinuclear space, although capsids accumulated in the nucleus; (iv) both UL47 and p32 were detected in primary enveloped virions in the perinuclear space by immunoelectron microscopy; (v) p32 knock-down induced aberrant membranous invaginations

containing primary enveloped virions adjacent to the nuclear membrane, which protruded into the nucleoplasm; and (vi) p32 knock-down together with the UL47-null mutation significantly reduced HSV-1 replication, although this effect was considerably attenuated in the absence of either. These results suggested that: (i) UL47 mediated the redistribution of p32 to the nuclear membrane and formed a complex with p32 and with UL31, UL34 and Us3, and (ii) UL47 and p32 played regulatory roles in primary envelopment and de-envelopment, respectively, and acted to promote HSV-1 replication in the same pathway, probably in the viral nuclear egress pathway.

Introduction

Viruses classified into the family *Herpesviridae* are called herpesviruses and a large family of DNA viruses that cause a series of diseases in animals and humans, such as cold sores around the mouth, Herpes stromal keratitis, encephatitis, genital herpes, chickenpox, infectious mononucleosis (Ann M. A and Don, 2013; Bernard et al., 2013; Philip E and Bernard, 2013). There are four important biological properties in common in all the herpesviruses. First, herpesviruses contain a large number of enzymes. These enzymes are needed in the metabolism of nucleic acid, viral DNA synthesis and modification of viral and cellular proteins. Second, viral DNA replication and transcription, nucleocapsid assembly, and encapsidation of virus genomes into progeny capsid take place in the nucleus. Third, the productive viral replication generally destroys the infected cells. Forth, all the herpesviruses have evolved mechanisms to persist in the certain host cell types for a long life (latent infection) (Philip E and Bernard, 2013). Apart from these common features, herpesviruses are different in many biological properties. Based on their differences, herpesviruses are divided into three subfamilies named the *Alpha-herpesvirinase*, *Beta-herpesvirinae*, and *Gamma-herpesvirinae*. They differ largely in host range, tissue tropism, replication

kinetics, clinical symptoms and disease severity (Kramer and Enquist, 2013; Philip E and Bernard, 2013). To date, eight human herpesviruses have been identified: herpes simplex virus 1 (HSV-1), herpes simplex virus 2 (HSV-2), varicella-zoster virus (VZV), Epstein-Barr virus (EBV), human cytomegalovirus (HCMV), human herpesvirus 6 (HHV-6), human herpesvirus 7 (HHV-7), and Kaposi's sarcoma-associated herpesvirus (KSHV) (Philip E and Bernard, 2013). Among them, HSV-1, HSV-2 and VZV belong to the *Alpha-herpesvirinae*, and have a relatively short replication life cycle and variable host range. They can efficiently destroy infected cells and establish latent infections in the sensory ganglia (Ann M. A and Don, 2013; Bernard et al., 2013). HCMV, HHV-6 and HHV-7 belong to the *Beta-herpesvirinae*, and have a long replication life cycle and a narrow host range. Latent infections are established in the white cells of the blood, secretory glands, kidneys, and other tissues (Edward S. M et al., 2013; Koichi. Y et al., 2013). EBV and HHV-8 belong to the *Gamma-herpesvirinae*, and are particular to infect B lymphocytes. It has also been demonstrated that the latency of the viruses is often in lymphoid tissues (Blossom A. D and C., 2013; Richard M et al., 2013).

The herpesvirus virions consist of four sections from inner to exterior: a linear double-stranded viral DNA genome core, where the length of the herpesvirus genome varies approximately from 124 to 295 k bp, an icosahedral capsid containing the viral DNA genome, a layer of tegument containing a more than 20 different viral unstructured proteins, and a lipid bilayer envelope containing a large number of glycoprotein splikes (Philip E and Bernard, 2013) (Fig 1A). In this thesis, we focus on HSV-1. The life cycle of HSV-1 includes lytic infection and latent infection. During lytic infection, HSV-1 infects epithelial cells in the mucous surface or at a break in the skin. Infections start when the viral particles bind to the cell surface through specific receptors. After binding, HSV-1 enters into the cell via two pathways. The first pathway is that HSV-1 envelope fuses directly with the plasma membrane at the cell surface. Another pathway is that HSV-1 is up-taken by endocytosis and viral envelope fuses with the endocytosis membrane in the cytoplasm (Bernard et al., 2013). Following HSV-1 entry into the cell, capsids latch onto microtubules and are then transported along microtubules to the nuclear pore. Once the incoming nucleocapsid binds to the nuclear pore complex, the viral DNA genome is released into the nucleus. During this process, a fraction of viral tegument proteins are dissociated from the

nucleocapsid (Bernard et al., 2013). They modulate the host cell or hijack cellular machinery to create the environment beneficial for efficient virus replication. For example, an endonuclease encoded by UL41 (VHS) tegument protein of HSV-1 degrades host mRNAs and induces host-cell shut off (Kwong and Frenkel, 1989). Another tegument protein UL48 (VP16) is tranlocated into the nucleus, forms a multi-protein complex with host cellular transcription factors including HCF1 and Oct-1, and then initiates the transcription of viral genes as a transactivator (Batterson et al., 1983; Johnson et al., 1999). The transcription and expression of viral genes are coordinately and sequentially regulated in a caspase fashion. HSV-1 genes are divided into three groups, named α, β and γ genes, based on the temporality of transcriptional regulation. Immediately after the linear viral DNA circularizes in the nucleus. α genes are transcribed by host cellular RNA polymerase Ⅱ to αmRNAs w

as described above. α mRNAs are exported to the cyptoplasm and translated into α proteins (Bernard et al., 2013). Synthysized α proteins translocate into the nucleus and transactivate β gene transcriptions, and then β proteins are synthesized. Most of β proteins are involved in viral DNA replication. The viral DNA is synthesized by a rolling circle mechanism. Circular concatemers are made and then are cleaved into

monomers to form linear chains of individual molecules (Bernard et al., 2013). After viral DNA replication, the γ genes are transcribed in large amounts, thereby leading to the synthesis of viral DNA.γ proteins are structural proteins and mainly involved in virion maturation pathway. After the progeny capsid is assembled, the linear viral genome is then inserted into newly assembled capsid cross over the portal by using a kind of terminase which have a robust ATPase-driven motor activity. After encapsidation of viral DNA into assembled capsid, viral protease activity is activated and capsid undergoes massive conformational changes from roughly and fragile spherical to a stable and icosahedral form (Baines, 2011; Bernard et al., 2013). The filled capsids go through the nuclear membranes. Capsids in the cytoplasm are decorated with tegument proteins, bud into vesicles derived from trans-Golgi network, and are then transported in vesicles to the plasma membrane. The vesicles fuse with the plasma membrane and finally the mature virions are released to the extracellular space (Bernard et al., 2013; Johnson and Baines, 2011; Mettenleiter et al., 2013) (Fig 1B). During latent infection, HSV-1 infects neurones and establishes latency at sensory ganglia. There is no cytopathic effect in this latently-infected cell. Viral DNA exists in a circular episomal form in the nucleus . Latency associated transcripts (LATs) are

highly expressed, whereas expression of most lytic genes is suppressed. Replicating viruses can not be detected (Bernard et al., 2013; Knipe and Cliffe, 2008). But sometimes, the virus is reactivated and replicates in the neurons. The infectious virus is taken by antergrade axonal transport to cells at or near the site of intial infection for recurrent infection (Bernard et al., 2013; Knipe and Cliffe, 2008; Philip E and Bernard, 2013). Several agents seem to trigger this reactivation. Stress related factors are considered to be most significant agents. For example, long time exposure to strong sunlight and fever can be factors for its recurrence. Perhaps, these related factors can suppress the host cell immune responses and lead to reactivation of virus proliferation in the nerve cell (Bernard et al., 2013; Philip E and Bernard, 2013).

As described above, morphogenesis of herpesviruses takes place in two different cellular compartments (Johnson and Baines, 2011; Mettenleiter et al., 2013). Viral DNA replication and transcription, capsid assembly, and packaging of nascent progeny virus genomes into preformed capsids take place in the nucleus, and final envelopment takes place in the cytoplasm (Johnson and Baines, 2011; Mettenleiter et al., 2013). Since herpesvirus nucleocapsids are too large to traverse the nuclear lamina or cross the inner and outer nuclear membranes (INM and ONM) through

nuclear pores, these viruses appear to have evolved a unique nuclear egress mechanism in which progeny nucleocapsids acquire primary envelopes by budding through the INM into the space between the INM and ONM, the perinuclear space, and enveloped nucleocapsids then fuse with the ONM to release de-enveloped nucleocapsids into the cytoplasm (Johnson and Baines, 2011; Mettenleiter et al., 2013). Although this type of vesicle-mediated nucleocytoplasmic transport has not been reported previously, other than for herpesvirus nuclear egress, it has recently been reported that cellular ribonucleoprotein complexes of *Drosophila* utilize a similar mechanism for their nucleocytoplasmic transport (Speese et al., 2012). This suggested that vesicle-mediated nucleocytoplasmic transport may be a general cellular mechanism for export of RNP complexes and other large macromolecular complexes from the nucleus.

HSV-1 is one of the best characterized members of the *Alphaherpesvirinae*, the neurotropic subfamily of herpesviruses. A heterodimeric complex of HSV-1 proteins UL31 and UL34, which are conserved all known herpesviruses, is critical for nuclear egress of herpesviruses and has been designated the nuclear egress complex (NEC) (Bernard et al., 2013; Johnson and Baines, 2011; Mettenleiter et al., 2013;

Reynolds et al., 2001; Roller et al., 2000). In the absence of the HSV-1 UL31/UL34 complex, nucleocapsids accumulate in the nucleoplasm, and progeny virus intermediates and virions are barely detectable in the perinuclear space, cytoplasm, or at the cell surface (Chang et al., 1997; Roller et al., 2000), indicating that the UL31/UL34 complex plays an essential role in primary envelopment of nucleocapsids, which is the first step in viral nuclear egress. The HSV-1 UL31/UL34 complex and its homologs in other herpesviruses have been suggested to coordinate multiple events in the primary envelopment of nucleocapsids, including: (i) disruption of the nuclear lamina by recruiting cellular protein kinases, such as protein kinase C (PKC), and by direct binding to components of the nuclear lamina (i.e., lamins A and C) and modifying their conformation (Bjerke and Roller, 2006; Johnson and Baines, 2011; Mettenleiter et al., 2013; Mou et al., 2007; Mou et al., 2008; Park and Baines, 2006; Reynolds et al., 2004); (ii) recruitment of nucleocapsids into primary envelopes by interaction of the UL31/UL34 complex and the capsid vertex specific component (CVSC), which consists of the conserved capsid proteins UL17 and UL25 (Toropova et al., 2011; Yang and Baines, 2011); and (iii) budding of capsids into the INM (Desai et al., 2012; Klupp et al., 2007).

In the second step of viral nuclear egress, de-envelopment of nucleocapsids, the primary envelopes of perinuclear virions need to fuse with the ONM to translocate nucleocapsids from the perinuclear space to the cytoplasm (Johnson and Baines, 2011; Mettenleiter et al., 2013). HSV-1 envelope glycoprotein B (gB) and the gH/gL heterodimer, which are all essential for virion fusion with the cell membrane during HSV-1 entry, have been proposed to also play roles in de-envelopment of nucleocapsids during nuclear egress. Thus, it has been reported that, in cells infected with mutant HSV-1 lacking both gB and gH, primary enveloped virions accumulated aberrantly in the perinuclear space and in membranous structures that were invaginations of the INM into the nucleoplasm (Farnsworth et al., 2007). Aberrant accumulation of primary enveloped virions in membranous invagination structures was also observed in the absence of the viral serine/threonine protein kinase Us3 or its catalytic activity in HSV-1-infected cells (Reynolds et al., 2002; Ryckman and Roller, 2004), suggesting that Us3 kinase activity also functioned in de-envelopment of nucleocapsids. It has been reported that Us3 phosphorylates UL31 and the cytoplasmic tail of gB, and that blocking Us3 phosphorylation of both UL31 and gB in combination with the null-mutation in gH induced membranous invagination structures containing

primary enveloped virions (Kato et al., 2009; Mou et al., 2009; Wisner et al., 2009), suggesting that Us3 phosphorylation of these substrates modulates perinuclear fusion during de-envelopment of nucleocapsids. Since Us3 phosphorylates and regulates proper localization of UL34 and UL31 at the nuclear membrane (Kato et al., 2005; Purves et al., 1991; Reynolds et al., 2001) and phosphorylates and modifies lamins A and C (Bjerke and Roller, 2006; Mou et al., 2007; Mou et al., 2008), Us3 also appears to be involved in primary envelopment of nucleocapsids. In addition to gB, gH/gL, Us3, and UL31, the VP16 and UL51 structural proteins in the virion tegument, the proteinaceous layer surrounding the nucleocapsid, and torsinA, a ubiquitously expressed cellular ATPase, have been suggested to be involved in HSV-1 de-envelopment: primary enveloped virions accumulate in the perinuclear space of cells with either a disrupted torsinA function or infected with HSV-1 mutants lacking VP16 or UL51 (Maric et al., 2011; Mossman et al., 2000; Nozawa et al., 2005). Thus, although several HSV-1 and cellular regulatory molecules and their roles in HSV-1 nuclear egress have gradually been elucidated, the precise mechanisms by which these HSV-1 and cellular proteins act in this process remain largely unknown. Furthermore, identification and characterization of additional viral and cellular regulatory

molecules/factors in HSV-1 nuclear egress appear to be needed for a more complete understanding of this process.

UL47 is a major structural protein in the HSV-1 virion tegument (Loret et al., 2008). It has been suggested that UL47 may be a positive regulator of viral replication and pathogenicity, based on studies showing that recombinant UL47 mutant viruses have reduced growth in cell cultures and reduced pathogenicity in a mouse model (Kato et al., 2011; Zhang et al., 1991). UL47 is an RNA binding protein (Donnelly et al., 2007) and shuttles between the cytoplasm and nucleus in infected cells (Donnelly and Elliott, 2001). It has been reported that UL47 can regulate subcellular localization of some viral and cellular proteins that interact with it. For example, UL47 together with the HSV-1 regulatory protein ICP27 associate with and promote nuclear translocation of the major form of the polyadenylate-binding protein PABC1 (Dobrikova et al., 2010), and UL47 forms a complex with and promotes nuclear localization of Us3 in infected cells (Kato et al., 2011). In a reciprocal process, Us3 was shown to phosphorylate UL47 and promote its nuclear localization (Kato et al., 2011). In cells infected with a mutant HSV-1 encoding a Us3 kinase-dead mutant or carrying a mutation in the Us3 phosphorylation site in UL47,

UL47 accumulated aberrantly at the nuclear membrane (Kato et al., 2011). UL47 was also shown to interact with capsid protein UL17 (Scholtes et al., 2010). As described above, UL17 forms a CVSC complex with UL25, which was suggested to recruit nucleocapsids for primary envelopment by interacting with the NEC (Toropova et al., 2011; Yang and Baines, 2011). Recently, it has been reported that UL47 interacted with the viral endoribonuclease responsible for virus host protein synthesis shutoff (vhs) and attenuated vhs activity (Shu et al., 2013). In this study, to clarify the role(s) of UL47 in HSV-1-virus-infected cells, we attempted to identify cellular proteins that interacted with UL47 by tandem affinity purification of transiently expressed UL47 coupled with mass spectrometry-based proteomics technology. We then focused on p32, which is also known as C1qBP, TAP and HABP, one of the putative UL47-interacting cellular proteins.

The p32 cell protein is primarily localized in the mitochondrial matrix, but has also been reported to be present at the cell surface and in the nucleus and cytoplasm (Brokstad et al., 2001; van Leeuwen and O'Hare, 2001). p32 is considered to be a multi-compartmental protein capable of interacting with a wide range of cellular proteins, such as the lamin B receptor, transcription factor TFIIB, high molecular

weight kininogen, protein kinase C, hyaluronic acids, proapoptotic factor HRK and tumor suppressor ARF (Itahana and Zhang, 2008; Lim et al., 1998; Lu et al., 1999; Robles-Flores et al., 2002; Rubinstein et al., 2004; Simos and Georgatos, 1994; Sunayama et al., 2004; Yu et al., 1995). In addition, p32 has been reported to interact with a wide variety of viral proteins, such as human immunodeficiency virus Rev (Luo et al., 1994) and Tat (Berro et al., 2006), an adenovirus core protein (Matthews and Russell, 1998), rubella virus capsid and replicase proteins (Beatch et al., 2005; Suppiah et al., 2012), a hepatitis C virus core protein (Kittlesen et al., 2000), Epstein-Barr virus (EBV) EBNA-1 (Van Scoy et al., 2000), HSV-1 ICP27 and ORF P (Bruni and Roizman, 1996; Bryant et al., 2000), human cytomegalovirus (HCMV) UL97, UL50 and UL53 (Marschall et al., 2005; Milbradt et al., 2009), herpesvirus saimiri (HVS) ORF73 (Hall et al., 2002) and murine gammaherpesvirus 68 (MHV-68) M2 (Liang et al., 2004). The ubiquity of p32 interactions with these viral proteins suggested its importance in the replication of diverse viruses. However, the biological significance of these interactions in the context of viral infections mostly remains to be determined. HSV-1 infection and overexpression of HSV-1 protein ICP27 have each been reported to cause redistribution of p32 to the nucleus (Bryant et al., 2000). Thus, although

some HSV-1 proteins have been reported to interact with p32 and one of them, ICP27, appeared to regulate subcellular localization of p32, the role(s) of p32 in HSV-1 replication remains largely unknown at present.

In this study, we investigated the effect of the interaction between p32 and UL47 in HSV-1-infected cells. The data presented here suggested that: (i) UL47 mediated redistribution of p32 to the nuclear membrane and formed a complex with p32, and with UL31, UL34 and Us3 in HSV-1-infected cells; and (ii) UL47 and p32 played regulatory roles in primary envelopment and de-envelopment, respectively, and promoted viral replication.

Materials and methods

Cells and viruses. Vero, rabbit skin and HEp-2 cells were described previously (Sugimoto et al., 2008; Tanaka et al., 2003). The HSV-1 wild-type strain HSV-1(F); recombinant virus YK511, encoding an enzymatically inactive Us3 mutant in which lysine at Us3 position 220 was replaced with methionine (Us3K220M); recombinant virus YK513, in which the Us3K220M mutation in YK511 was repaired (Us3K220M-repair); recombinant virus YK524, encoding UL47 fused to the fluorescent protein mRFP1 (mRFP1-UL47); recombinant virus YK527, encoding mRFP1-UL47 and carrying the Us3K220M mutation (mRFP1-UL47/Us3K220M); recombinant virus YK528, in which Us3K220M in YK527 was repaired (mRFP1-UL47/Us3K220M-repair); recombinant virus YK523, encoding mRFP1-UL47 and Us3 fused to the fluorescent protein VenusA206K; recombinant virus YK545, a UL47-null mutant virus in which the UL47 gene was disrupted by insertion of a foreign gene cassette just downstream of the UL47 start codon (ΔUL47); and recombinant virus YK546, in which the foreign gene cassette inserted into the UL47 locus of YK545 (ΔUL47) was excised (ΔUL47-repair) have been described previously (Kato et al., 2011; Kato et al., 2008) (Fig. 2).

Plasmids. Plasmids were constructed for this study as follows (Fig. 2). (i) Plasmids were constructed for this study as follows (Fig. 2). (i) To construct pcDNA-MEF-UL47, an expression plasmid for UL47 fused to an MEF tag (MEF-UL47), the UL47 ORF without a start codon was amplified by PCR from pBC1007 (Kawaguchi et al., 1997) and cloned into pcDNA-MEF (Arii et al., 2010). (ii) pcDNA-MEF-gB, an expression plasmid for gB fused to an MEF tag (MEF-gB), was constructed by cloning a DNA fragment encoding MEF-gB amplified by PCR from viral DNA of a recombinant virus expressing MEF-gB (Arii et al., 2010) into pcDNA4/HisMax C (Invitrogen). (iii) pGEX-p32, for generating a fusion protein of glutathione *S*-transferase (GST) and p32, was constructed by amplifying the entire p32 coding sequence by PCR from an EBV-transformed human peripheral blood lymphocyte MATCHMAKER cDNA library (Clontech) in frame with GST. (iv) pCMV-p32(F), an expression plasmid for p32 fused to three Flag tag repeats at its C-terminus [p32(F)], was constructed by cloning the entire p32 coding sequence without a stop codon amplified by PCR from pGEX-p32 into p3xFlag-CMV-14 (Sigma). (v) To generate a fusion protein of maltose binding protein (MBP) and either p32, part of HSV-1 UL31 or part of HSV-2 UL31, plasmid pMAL-p32,

pMAL-UL31-C or pMAL-UL31(2)-Pii, respectively, was constructed by cloning the entire coding sequence of p32 without a start codon amplified by PCR from pGEX-p32, the HSV-1 UL31 domain encoding codons 50-307 amplified by PCR from pBC1007 or the HSV-2 UL31 domain encoding codons 183-306 amplified by PCR from pYEbac356, a full-length infectious HSV-2 186 clone (Morimoto et al., 2009), respectively, into pMAL-c (New England BioLabs) in frame with the MBP. (vi) To generate fusion proteins of MBP and parts of UL47, plasmids pMAL-UL47-Pi, pMAL-UL47-Pii and pMAL-UL47-Piii were constructed by cloning the UL47 domain encoding codons 1-120, 121-390 or 380-693, respectively, amplified by PCR from pBC1007 into pMAL-c. (vii) To construct pBS-EGRp-MEF-polyA-Kan, the plasmid used for generating YK761 carrying an expression cassette consisting of the Egr-1 promoter, MEF tag and bidirectional polyadenylation signals of the HSV-1 UL21 and UL22 genes (EGRp-MEF-polyA) in the intergenic region between the UL50 and UL51 genes (Wt/MEF) (Fig. 2), the pGEM-MEF domain (Arii et al., 2010) encoding the I-*Sce*I site, an MEF tag and the kanamycin resistance gene was amplified by PCR from pGEM-MEF using primers 5'-GCACTAGTATGGAGCAAAAGCTCATTTC-3' and 5'-GCACTAGTTTAATCTTTGTCATCGTCGTCCT-3' and cloned into the *Spe*I site of

pRB5160, which contained the Egr-1 promoter region, multicloning site, and bidirectional polyadenylation signals of the HSV-1 UL21 and UL22 genes (Kato et al., 2014; Kawaguchi et al., 1997). (viii) To generate pGEX-p32-Kan, the plasmid used for generating recombinant virus YK537, carrying an expression casette consisting of the Egr-1 promoter, MEF-tagged p32 ORF and bidirectional polyadenylation signals of the HSV-1 UL21 and UL22 genes in the intergenic region between UL50 and UL51 (MEF-p32) (Fig. 2), was constructed by cloning the domain encoding the I-*Sce*I site and a kanamycin resistance gene amplified by PCR from pEPkan-S (Kato et al., 2008) using primers 5'-GCGAGCTCAGCACAGCCCTGGAGCACCAAGGATGACGACGATAAGTAGG G-3' and 5'-GCGAGCTCCACCAGCTCATCTGCAAAAGCAACCAATTAACCAATTCTGAT TAG-3' into the *Sac*I site of pGEX-p32. (ix) pSSCH-p32, for generating a stable cell line expressing shRNA against the 3'-UTR of p32 mRNA, was constructed as follows. Oligonucleotides 5'-TTTGATTATCATCCTAATATCATGGCTTCCTGTCACCATGATATTAGGATGAT AATCTTTTTTG-3' and

5’-AATTCAAAAAAGATTATCATCCTAATATCATGGTGACAGGAAGCCATGATA TTAGGATGATAAT -3’ were annealed and cloned into the *Bbs*I and *Eco*RI sites of pmU6 (Arii et al., 2010). The *Bam*HI-*Sal*I fragment of the resultant plasmid, containing the U6 promoter and the sequence encoding shRNA against the 3’-UTR of p32, was cloned into the *Bam*HI and *Sal*I sites of pSSCH, which is a derivative of the retrovirus vector pMX containing a hygromycin B resistance gene, to produce pSSCH-p32. (x) Plasmid pSSCH-Luc encoding shRNA against firefly luciferase (Luc) mRNA was constructed by the same procedure as pSSCH-p32, except using oligonucleotides 5′-TTTGTCAAATGGCGATTACCGTTGGCTTCCTGTCACCAACGGTAATCGCCA TTTGACTTTTTTG-3′ and 5′-AATTCAAAAAAGTCAAATGGCGATTACCGTTGGTGACAGGAAGCCAACG GTAATCGCCATTTGA -3′ (Kato et al., 2014). (xi) pMXs-p32, a retrovirus vector expressing p32, was constructed by cloning the entire p32 coding sequence amplified by PCR from pGEX-p32 into pMXs-puro (Arii et al., 2010).

Identification of proteins that interact with UL47. 293T cells were transfected with pcDNA-MEF or pcDNA-MEF-UL47 using polyethylenimine as

described previously (Maruzuru et al., 2013), harvested at 48 h post-transfection, and lysed in 0.1% NP-40 buffer (50 mM Tris-HCl [pH 8.0], 120 mM NaCl, 50 mM NaF, 0.1% NP-40) containing a protease inhibitor cocktail (Nacalai Tesque). After centrifugation, the supernatants were immunoprecipitated with an anti-Myc monoclonal antibody and the immunoprecipitates were incubated with AcTEV protease (Invitrogen). After another centrifugation, the supernatants were immunoprecipitated with an anti-Flag monoclonal antibody and the immunoprecipitates were washed three times with wash buffer (50 mM Tris-HCl [pH 8.0], 120 mM NaCl, 50 mM NaF). The immunoprecipitates were analyzed by electrophoresis in 7.5% and 12% denaturing polyacrylamide gels and visualized by silver staining (Daiichikagaku, Japan) according to the manufacturer's instructions. Protein bands from cells transfected with pcDNA-MEF-UL47, but not with pcDNA-MEF (Fig. 3), were excised from the denaturing gels, digested in the gel with trypsin, and analyzed by nano liquid chromatography tandem mass spectrometry (nanoLC-MS/MS) as described previously (Arii et al., 2010). For this analysis, we used Q-STAR Elite (AB SCIEX) coupled with Dina (KYA Technologies). The MS/MS signals were then analyzed against the human proteins in the RefSeq database

(National Center for Biotechnology Information; 35,853 sequences as of February 4, 2013) using the Mascot algorithm (Version 2.4.1; Matrix Science) with the following parameters: variable modifications, oxidation (Met), protein N-terminal acetylation, pyroglutamination (Gln); maximum missed cleavages, 2; peptide mass tolerance, 200 ppm; and MS/MS tolerance, 0.5 Da. Protein identification was based on the criterion of having at least one MS/MS data signal with a Mascot score greater than the threshold ($P < 0.05$).

Mutagenesis of viral genomes in *Escherichia coli* and generation of recombinant HSV-1. To generate recombinant viruses YK536 (MEF-UL47), YK538 (MEF-UL34) and YK539 (MEF-UL31) (Fig. 2), a two-step Red-mediated mutagenesis procedure was carried out using *E. coli* GS1783 containing pYEbac102 (Tanaka et al., 2003) and a full-length infectious HSV-1(F) clone, as described previously (Kato et al., 2008) except with the primers listed in Table 5. To construct YK761 (Wt/MEF), the two-step Red-mediated mutagenesis procedure was carried out as described previously (Kato et al., 2014; Kato et al., 2008), except with the primers listed in Table 5 and pBS-EGRp-MEF-polyA-Kan. YK537 (MEF-p32) was constructed by the two-step Red-mediated mutagenesis procedure as described above,

except with the primers listed in Table 5, pGEX-p32-Kan and *E. coli* containing a YK761 genome.

Production and purification of MBP and GST fusion proteins in *E. coli*. MBP fusion proteins MBP-p32, MBP-UL31-C, MBP-UL31(2)-Pii, MBP-LacZ, MBP-UL47-Pi, MBP-UL47-Pii and MBP-UL47-Piii, and GST fusion protein GST-p32 were expressed in E. coli that had been transformed with pMAL-p32, pMAL-UL31-C, pMAL-UL31(2)-Pii, pMAL-c, pMAL-UL47Pi, pMAL-UL47Pii, pMAL-UL47Piii or pGEX-p32, respectively, and purified as described previously (Kato et al., 2005; Kawaguchi et al., 1997).

Antibodies. To generate rabbit polyclonal antibody to p32, UL31 or UL47, rabbits were immunized with purified GST-p32, MBP-UL31(2)-Pii or a mixture of MBP-UL47-Pi, pMAL-UL47Pii and pMAL-UL47Piii, respectively, as described previously (Sugimoto et al., 2008). Serum from the immunized rabbits was used as anti-p32, anti-UL31 or anti-UL47 rabbit polyclonal antibody. To generate mouse polyclonal antibody to UL31, BALB/c mice were immunized once with purified MBP-UL31C with TiterMax Gold (TiterMax USA, Inc. Serum from the immunized mice was used as anti-UL31 mouse polyclonal antibody. Commercial mouse

monoclonal antibodies against Flag (M2, Sigma), Myc (PL14, MBL), VP5 (3B6, Virusys), ICP8 (10A3, Chemicon) and β-actin (AC15, Sigma) were used in this study. Rabbit polyclonal antibody to UL34 and chicken polyclonal antibody to UL34 were described previously (Kato et al., 2008; Morimoto et al., 2009).

Ethics statement. All animal experiments were carried out in accordance with the Guidelines for Proper Conduct of Animal Experiments, Science Council of Japan. The protocol was approved by the Institutional Animal Care and Use Committee (IACUC) of the Institute of Medical Science, The University of Tokyo (IACUC protocol approval number: 19-26).

In vitro kinase assays. MBP fusion proteins were captured on amylose beads (New England BioLabs) and used as substrates in in vitro kinase assays with purified GST-Us3 and GST-Us3K220M as described previously (Kato et al., 2005).

Antibody analyses. Immunoprecipitation, immunoblotting and immunofluorescence were performed as described previously (Kawaguchi et al., 1997; Sugimoto et al., 2008).

Purification of virions. Vero cells were infected with wild-type HSV-1(F) at an MOI of 0.01 for 48 h. For purification of extracellular virions, cell culture

supernatants were harvested by low-speed centrifugation. For purification of total virions (i.e., extra- and intracellular virions), infected cells were subjected to three rounds of freezing and thawing and supernatants were harvested as described above. Extracellular and total virions were purified from the virion-containing supernatants as described previously (Sugimoto et al., 2008).

Generation of recombinant retroviruses and establishment of cell lines stably expressing shRNA against p32 and firefly luciferase. Recombinant retroviruses were generated as described previously (Arii et al., 2010). Briefly, sh-p32-HEp-2 and sh-Luc-HEp-2 cells were isolated from HEp-2 cells that were infected with retrovirus-containing supernatants of Plat-GP cells that had been transfected with pSSCH-p32 or pSSCH-Luc, respectively, and selected with 50 μg hygromycin B/ml (Kato et al., 2014).

Assay for cell viability. The viability of sh-Luc-HEp-2 and sh-p32-HEp-2 cells was determined using a Cell Counting Kit-8 (Dojindo) according to the manufacturer's instructions.

Establishment of sh-p32-HEp-2 cells expressing p32 exogenously and their control cells. sh-p32-HEp-2/p32(+) and sh-p32-HEp-2/Ct cells were isolated from

sh-p32-HEp-2 cells that were infected with retrovirus-containing supernatants of Plat-GP cells that had been transfected with pMXs-p32 or pMXs, respectively, and selected with 2 μg puromycin/ml.

Electron microscopic analysis. Vero cells infected with wild-type HSV-1(F), YK545 (ΔUL47) or YK546 (ΔUL47-repair) at an MOI of 5 for 18 h, and sh-Luc-HEp-2 and sh-p32-HEp-2 cells infected with wild-type HSV-1(F) at an MOI of 5 for 24 h were examined by ultrathin-section electron microscopy as described previously (Morimoto et al., 2009). Immunoelectron microscopy to detect p32 was performed as described previously (Noda et al., 2006; Noda et al., 2012). Briefly, Vero cells infected with wild-type HSV-1(F) or YK536 (MEF-UL47) at an MOI of 5 for 18 h were fixed with 2% paraformaldehyde and 1% glutaraldehyde in 0.1M cacodylate buffer (pH 7.4) on ice for 1 h. After a wash with the same buffer, the cells were post-fixed with 2% osmium tetroxide on ice for 1 h, washed with distilled water, dehydrated with an ethanol gradient series, incubated in propylene oxide, and embedded in an Epon 812 resin mixture. Ultrathin-sections were prepared on nickel grids as described previously (Noda et al., 2006) and incubated with a saturated sodium periodate solution (Noda et al., 2012), followed by 0.2 M glycine in PBS

buffer. After a PBS wash, the sections were incubated with 1% bovine serum albumin (BSA) in PBS, and then with anti-p32 rabbit polyclonal or anti-Myc mouse monoclonal antibody. The sections were then washed with PBS and incubated with goat anti-rabbit or anti-mouse IgG conjugated to 10-nm gold particles. After immunostaining, the sections were stained with 2% uranyl acetate and Reynold's lead citrate and examined by transmission electron microscopy.

Results

Identification of cell proteins that interact with UL47 and verification of UL47 interaction with p32. To identify host cell proteins that interact with UL47, we used tandem affinity purification coupled with mass spectrometry-based proteomics analysis. These experiments identified 14 cell proteins that co-imunoprecipitated with transiently expressed UL47 fused to an MEF tag with myc and Flag epitopes and a TEV protease cleavage site (MEF-UL47) (Fig. 3 and Table 1). Of these proteins, we focused on p32 in this study. To verify and extend the interaction data obtained with mass spectrometry-based proteomics screening, we performed two series of experiments. In the first series of experiments, 293T cells were mock-transfected or transfected with pCMV-p32(F) expressing Flag-tagged p32 alone, with pcDNA-MEF-UL47 expressing MEF-tagged UL47 alone, or with pCMV-p32(F) in combination with either pcDNA-MEF-UL47 or pcDNA-MEF-gB expressing MEF-tagged gB. The cells were lysed 2 d post-transfection and immunoprecipitated with anti-Myc antibody, and the immunoprecipitates were analyzed by immunoblotting with anti-Flag antibody. As shown in Fig. 4, anti-Myc antibody co-precipitated Flag-tagged p32 from cells co-transfected with MEF-tagged UL47 but not with

MEF-tagged gB. These results not only confirmed the interaction between UL47 and p32 in transfected cells, but also indicated that UL47 interacted with p32 in the absence of other HSV-1 proteins. In the second series of experiments, Vero cells infected with YK536 (MEF-UL47) encoding MEF-tagged UL47 (Fig. 2) or wild-type HSV-1(F) were lysed at 18 h post-infection and immunoprecipitated with anti-Flag antibody, and the immunoprecipitates were analyzed by immunoblotting with anti-p32 antibody. In addition, Vero cells infected with YK537 (MEF-p32) expressing MEF-tagged p32 (Fig. 2) or wild-type HSV-1(F) were lysed at 18 h post-infection and immunoprecipitated with anti-Flag antibody, and the immunoprecipitates were analyzed by immunoblotting with anti-UL47 antibody. As shown in Fig. 5, anti-Flag antibody co-precipitated endogenous p32 with MEF-tagged UL47 from lysates of YK536 (MEF-UL47)-infected Vero cells and also co-precipitated UL47 with MEF-tagged p32 from lysates of YK537 (MEF-p32)-infected Vero cells. These results indicated that UL47 formed a complex with p32 in HSV-1-infected cells.

Effect of p32 on HSV-1 replication in the presence or absence of UL47. To investigate the role(s) of p32 in HSV-1 replication, we generated HEp-2 cell lines stably expressing shRNA against the 3'-UTR of p32 mRNA (sh-p32-HEp-2) to

knock-down p32 expression, and a control cell line (sh-Luc-HEp-2) expressing shRNA against firefly luciferase mRNA. As shown in Fig. 6A, expression of endogenous p32 protein in sh-p32-HEp-2 cells was considerably less than in sh-Luc-HEp-2 cells. In contrast, the viability of sh-p32-HEp-2 cells was similar to that of sh-Luc-HEp-2 cells, indicating that p32 knock-down was not lethal to HEp-2 cells (Fig. 6B). sh-p32-HEp-2 and sh-Luc-HEp-2 cells were then infected with wild-type HSV-1(F) at an MOI of 0.01, and viral titers were determined at various times post-infection. As shown in Fig. 6C, progeny virus titers in sh-p32-HEp-2 cells were significantly (12.9- to 33.3-fold) lower than in sh-Luc-HEp-2 cells at all post-infection times tested. To eliminate the possibility that the reduced viral replication observed in sh-p32-HEp-2 cells was due to a non-specific effect(s) of the shRNA, we generated sh-p32-HEp-2/p32(+) cells in which p32 was expressed exogenously, by transduction of sh-p32-HEp-2 cells with a retrovirus vector expressing p32, and control sh-p32-HEp-2/Ct cells in which sh-p32-HEp-2 cells were transduced by the empty retrovirus vector (Fig. 7A). As shown in Fig. 7B, the progeny virus yield in sh-p32-HEp-2/p32(+) cells was restored to the level in sh-Luc-HEp-2 cells. These results indicated that p32 was required for efficient HSV-1 replication in cell cultures.

Next, we compared the effects of p32 knock-down on viral replication in the presence and absence of UL47. For these studies, sh-p32-HEp-2 and sh-Luc-HEp-2 cells were infected with wild-type HSV-1(F), the UL47-null mutant virus YK545 (ΔUL47) or its repaired virus YK546 (ΔUL47-repair) (Fig. 2) at an MOI of 0.01, and viral titers were assayed 48 h post-infection. In agreement with the results in Fig. 6C, p32 knock-down reduced progeny virus titers in wild-type HSV-1(F)- and YK546 (ΔUL47-repair)-infected cells 19.0- and 15.0-fold, respectively, but only reduced the progeny virus titer in YK545 (ΔUL47)-infected cells 2-fold (Fig. 8). Also, in agreement with previous reports showing that the UL47-null mutation reduced viral replication in cell cultures (Kato et al., 2011), YK545 (ΔUL47) had a 25.0- and 22.5-fold lower progeny virus yield than wild-type HSV-1(F) and YK546 (ΔUL47-repair), respectively, in Sh-Luc-HEp-2 cells. However, YK545 (ΔUL47) only had a 2.7- and 3.1-fold lower progeny virus yield than wild-type HSV-1(F) and YK546 (ΔUL47-repair), respectively, in Sh-p32-HEp-2 cells (Fig. 8). In addition, as reported previously (Kato et al., 2011), the UL47-null mutation in YK545 (ΔUL47) had no effect on expression of the neighboring UL46 and UL48 genes (Fig. 9). These results indicated that the effects of p32 and UL47 on HSV-1 replication were mutually dependent on each other.

UL47 is required for the redistribution of p32 to the nuclear membrane in HSV-1-infected cells. To investigate the significance of the interaction between UL47 and p32 in HSV-1 infected cells, we examined the subcellular localization of p32 in the presence or absence of UL47 in infected cells. For these studies, Vero cells were mock-infected or infected with wild-type HSV-1(F), YK545 (ΔUL47), YK546 (ΔUL47-repair) or R7356 (ΔUL13), which has a null mutation in the HSV-1 UL13 protein kinase (Fig. 2), and p32 localization in the infected cells was analyzed by immunofluorescence microscopy. As reported previously (Bryant et al., 2000), p32 was detected predominantly in the cytoplasm of mock-infected cells (Fig. 10). However, in wild-type HSV-1(F)- and YK546 (ΔUL47-repair)-infected cells (Fig. 10), although still present in the cytoplasm, p32 was predominantly at the nuclear rim and co-localized with lamins A and C (Fig. 10B), which are nuclear membrane markers. Similarly, in Vero cells infected with R7356 (ΔUL13), p32 was predominantly localized at the nuclear membrane (Fig. 11). In contrast, p32 was detected predominantly in the cytoplasm of cells infected with YK545 (ΔUL47) (Fig. 10). We noted that p32 appeared to be distributed more diffusely in the cytoplasm of cells infected with YK545 (ΔUL47) than in mock-infected cells (Fig. 10). These results

indicated that UL47 was specifically required for the redistribution of p32 from the cytoplasm to the nuclear membrane in HSV-1-infected cells.

Interactions among p32, UL34, UL31, Us3 and UL47 in HSV-1-infected cells. The data above showing that p32 redistribution to the nuclear membrane in HSV-1-infection cells was UL47-dependent led us to investigate whether p32 alone, UL47 alone or a combination of p32 and UL47 regulated nuclear egress of viral nucleocapsids, since this event takes place at the nuclear membrane (Johnson and Baines, 2011; Mettenleiter et al., 2013). Therefore, we performed three series of experiments to examine whether, in HSV-1-infected cells, p32 and/or UL47 interacted with UL31, UL34 or Us3, all of which have been reported to be critical for viral nuclear egress (Johnson and Baines, 2011; Mettenleiter et al., 2013). In the first series of experiments, Vero cells were infected with wild-type HSV-1(F), YK536 (MEF-UL47), YK538 (MEF-UL34) encoding MEF-tagged UL34, or YK539 (MEF-UL31) encoding MEF-tagged UL31 (Fig. 2) and, at 18 h post-infection, were lysed, immunoprecipitated with anti-Myc antibody, and the immunoprecipitates were analyzed by immunoblotting with antibodies to the viral and cellular proteins shown in Fig. 12. As shown in Fig. 12A, anti-Myc antibody co-precipitated UL31, UL34, Us3,

VP5 and p32 with MEF-tagged UL47 from lysates of YK536 (MEF-UL47)-infected Vero cells, but did not co-precipitate VP23 or ICP8. In contrast, the anti-Myc antibody did not immunoprecipitate any of these viral and cellular proteins from lysates of wild-type HSV-1(F)-infected cells (Fig. 12A). These results indicated that UL47 formed a complex(es) with UL31, UL34, Us3, VP5 and/or p32 in HSV-1-infected cells. Similarly, anti-Myc antibody co-precipitated UL34, Us3, UL47 and p32 with MEF-tagged UL31 from lysates of YK539 (MEF-UL31)-infected cells (Fig. 12B), and co-precipitated UL31, UL47, Us3 and p32 with MEF-tagged UL34 from lysates of YK538 (MEF-UL34)-infected cells (Fig. 12C). These results indicated that UL31 formed a complex(es) with UL34, Us3, UL47 and/or p32, and UL34 formed a complex(es) with UL31, Us3, UL47 and/or p32 in HSV-1-infected cells.

In the second series of experiments, we examined whether p32 and UL47 co-localized with UL31, UL34 and Us3 at the nuclear membrane in HSV-1-infected cells. It has been noted by us and other laboratories that the anti-Us3 and anti-UL47 antibodies reported to date were not useful for immunofluorescence assays because they showed non-specific staining (Kato et al., 2011; Kato et al., 2008; Reynolds et al.,

2002; Scholtes et al., 2010). In agreement with these reports, the anti-UL47 and anti-Us3 antibodies used this study were not useful for immunofluorescence (data not shown). Therefore, we used YK523 (VenusA206A-Us3/mRFP1-UL47) expressing Us3 and UL47 tagged with fluorescent proteins VenusA206K and mRFP1 (Kato et al., 2011), respectively, to detect Us3 and UL47 localization (Fig. 2). Vero cells infected with YK523 (VenusA206A-Us3/mRFP-UL47) were fixed at 18 h post-infection, and stained with anti-UL34, UL31 or p32 antibody, to enable simultaneous localization of combinations of these proteins to be observed by confocal microscopy. As shown in Fig. 13, VenusA206-Us3 and mRFP1-UL47 co-localized with UL34, UL31 and p32 at the nuclear membrane in Vero cells infected with YK523 (VenusA206A-Us3/mRFP-UL47), indicating that these viral and cellular proteins co-localized at the nuclear membrane in HSV-1-infected cells.

As described above, Us3 has been reported to phosphorylate UL31, UL34 and UL47 (Kato et al., 2011; Kato et al., 2005; Purves et al., 1991), and to regulate their proper localization at the nuclear membrane in HSV-1-infected cells (Kato et al., 2011; Reynolds et al., 2001). In the absence of Us3 protein or its catalytic activity, these viral proteins were shown to localize aberrantly in punctate structures at the nuclear

membrane in HSV-1-infected cells (Kato et al., 2011; Reynolds et al., 2001). Therefore, in the third series of experiments, we examined whether p32 localization was also regulated by Us3 kinase activity in HSV-1-infected cells. Vero cells were infected with wild-type HSV-1(F), the Us3 kinase-dead mutant YK511 (Us3K220M) or its repaired virus YK513 (Us3K220M-repair) (Fig. 2), fixed at 18 h post-infection, and then stained with anti-p32 antibody in combination with anti-UL31 or anti-UL34 antibody and localization of these viral and cellular proteins was examined by confocal microscopy. In agreement with the results shown in Fig. 13, p32 co-localized with UL34 and UL31 at the nuclear membrane with a uniform distribution in Vero cells infected with wild-type HSV-1(F) or YK513 (Us3K220M-repair) (Fig. 14). In contrast, p32 was detected in punctate structures at the nuclear membrane in Vero cells infected with YK511 (Us3K220M) and co-localized with UL31 and UL34 in these structures (Fig. 14). Next, Vero cells were infected with YK524 (mRFP1-UL47) encoding mRFP1-UL47, YK527 (mRFP1-UL47/Us3K220M) encoding mRFP1-UL47 and Us3 with the kinase-dead K220M mutation, or YK528 (mRFP1-UL47/Us3K220M-repair) in which Us3 K220M mutation in YK527 was repaired (Fig. 2). At 18 h post-infection, infected cells were fixed, stained with

anti-p32, anti-UL34, or anti-UL31 antibody, and localization of mRFP1-UL47 in combination with p32, UL34 or UL31 was examined by confocal microscopy. As shown in Fig. 15, in Vero cells infected with YK527 (mRFP1-UL47/Us3K220M), mRFP1-UL47 accumulated in punctate structures at the nuclear membrane, in agreement with a previous report (Kato et al., 2011), and co-localized with UL34, UL31 and p32 in these structures at the nuclear membrane (Fig. 15). These results indicated that Us3 catalytic activity was required for proper localization, not only of UL31, UL34 and UL47, but also of p32 at the nuclear membrane in HSV-1-infected cells and suggested that localization of these viral and cellular proteins at the nuclear membrane was regulated by Us3 catalytic activity.

Us3 phosphorylation of p32 in vitro. It has been reported that UL34, UL31 and UL47 were substrates for Us3 (Kato et al., 2011; Kato et al., 2005; Purves et al., 1991). Therefore, we examined whether Us3 also phosphorylated p32, since (as described above) we had shown that p32 localization at the nuclear membrane in infected cells was regulated by Us3 catalytic activity, as UL31, UL34 and UL47 localization were (Fig. 14 and 15). Using the in vitro kinase assay we previously reported (Kato et al., 2005), purified enzymatically active GST-Us3 was shown to

phosphorylate full-length p32 fused to MBP, but not MBP-LacZ (Fig. 16). In agreement with previous reports (Kato et al., 2005), MBP-UL34 was efficiently phosphorylated by GST-Us3. When the purified kinase-dead mutant GST-Us3K220M was used, none of the MBP fusion proteins (i.e., LacZ, UL34 and p32) were phosphorylated. These results indicated that Us3 directly phosphorylated p32.

Effect of the UL47-null mutation on viral nuclear egress. To examine whether UL47 played a role(s) in HSV-1 nuclear egress, we investigated the effect of the UL47-null mutation on viral morphogenesis by quantitating the number of virus particles at different morphogenetic stages by electron microscopy of Vero cells infected with wild-type HSV-1(F), YK545 (ΔUL47) or YK546 (ΔUL47-repair). In Vero cells infected with wild-type HSV-1(F) or YK546 (ΔUL47-repair), 19.9 and 15.9%, respectively, of the total number of virus particles were primary enveloped virions in the perinuclear space (Table 2). However, cells infected with YK545 (ΔUL47) had almost no (0.4%) primary enveloped virions in the perinuclear space, which was 49.8- and 39.8-fold less than that in cells infected with wild-type HSV-1(F) or YK546 (ΔUL47-repair), respectively (Table 2 and Fig. 17). In contrast, capsids

appeared to accumulate in the nucleus in cells infected with YK545 (ΔUL47) (Table 2). While 34.1 and 38.3% of total virus particles were capsids in the nucleus in cells infected with wild-type HSV-1(F) or YK546 (ΔUL47-repair), respectively, the fraction of total virus particles that were capsids in the nucleus in cells infected with YK545 (ΔUL47) increased to 63.8% (Table 2). Similar results were also obtained with HEp-2 cells infected with wild-type HSV-1(F), YK545 (ΔUL47) or YK546 (ΔUL47-repair) (Table 3). These results indicated that the UL47-null mutation resulted in a decrease in the fraction of virus particles that were primary enveloped virions in the perinuclear space and an increase in the fraction that were capsids in the nucleus.

Effect of p32 knock-down on nuclear egress of wild-type virus. We next investigated viral morphogenesis in sh-p32-HEp-2 and sh-Luc-HEp-2 cells infected with wild-type HSV-1(F) by electron microscopy. Membranous invagination structures containing several primary enveloped virions were observed in the nucleoplasm adjacent to the nuclear membrane in sh-p32-HEp-2 cells (Fig. 18B), but not many were seen in sh-Luc-HEp-2 cells (Fig. 18A). Quantitation of these data showed a 21- and 25-fold increase in membranous invaginations and in enveloped

virions in membranous invaginations, respectively, in sh-p32-HEp-2cells compared to sh-Luc-HEp-2 cells (Table 4). Similar results were also found with sh-p32-HEp-2/Ct and sh-p32-HEp-2/p32(+) cells infected with wild-type HSV-1(F) (data not shown), eliminating the possibility that induction of the membranous invaginations containing primary enveloped virions in infected sh-p32-HEp-2 cells was due to a non-specific effect(s) of the shRNA. We also examined localization of UL31 and UL34 in sh-p32-HEp-2, sh-Luc-HEp-2, sh-p32-HEp-2/Ct and sh-p32-HEp-2/p32(+) cells infected with wild-type HSV-1(F) by immunofluorescence microscopy. As shown in Fig. 19A and Fig. 20A, UL31 and UL34 co-localized at the nuclear membrane and in punctate structures adjacent to the nuclear membrane, which protruded into the nucleoplasm in sh-p32-HEp-2 and sh-p32-HEp-2/Ct cells. The punctate structures were induced in a similar fraction of sh-p32-HEp-2 and sh-p32-HEp-2/Ct cells infected with wild-type HSV-1(F) (27.7% and 28.4%, respectively), but were barely detectable in sh-Luc-HEp-2 and sh-p32-HEp-2/p32(+) cells infected with wild-type HSV-1(F) (Fig. 19B and Fig. 20B). These results indicated that p32 knock-down induced membranous invagination structures containing primary enveloped virions adjacent to the nuclear membrane and aberrant localization of UL34 and UL31 in punctate

structures adjacent to the nuclear membrane.

Effect of p32 knock-down on nuclear egress of UL47-null mutant virus. To investigate the relationship between the effects of UL47 and p32 on HSV-1 nuclear egress, we first compared the effect of p32 knock-down on nuclear egress of nucleocapsids in the presence and absence of UL47 in infected cells. In agreement with the results in Fig. 18 and 19, p32 knock-down induced membranous invaginations containing primary enveloped virions in the nucleoplasm adjacent to the nuclear membrane (data not shown) and aberrant localization of UL31 and UL34 in punctate structures adjacent to the nuclear membrane in cells infected with wild-type HSV-1(F) or YK546 (ΔUL47-repair) (Fig. 21 and Fig. 22). In contrast, p32 knock-down barely induced these structures in YK545 (ΔUL47)-infected cells (Fig. 21, Fig. 22 and data not shown). These results indicated that UL47 was required for p32 knock-down induction of aberrant membranous invagination structures at the nuclear membrane and aberrant localization of UL34 and UL31 in punctate structures at the nuclear membrane.

We next compared the effect of the UL47-null mutation on nuclear egress of nucleocapsids in sh-Luc-HEp-2 and sh-p32-HEp-2 cells. These results showed that the UL47-null mutation reduced the fraction of virus particles in primary enveloped

virions in the perinuclear space and in the membranous invagination structures, and capsids accumulated in the nucleus at similar levels in sh-Luc-HEp-2 and HEp-2 cells (data not shown). These results suggested that the effects of UL47 on HSV-1 nuclear egress were independent of the presence of p32.

Localization of p32 and UL47 in infected cells by immunoelectron microscopy. UL31, UL34 and Us3 have been reported to localize at the nuclear membrane and to be components of primary enveloped virions in the perinuclear space, and Us3 to localize at cytoplasmic membranes and extra-nuclear virions (Reynolds et al., 2002). To localize p32 and UL47 in HSV-1-infected cells at the ultra-structural level, Vero cells infected with wild-type HSV-1(F) were examined by immunoelectron microscopy using anti-p32 serum to detect p32. Pre-immune serum of the rabbit used to generate anti-p32 serum was used as a negative control and was barely detected in mock- and wild-type HSV-1(F)-infected cells (data not shown). As shown in Fig. 23A, the p32-specific antibody localized at the nuclear membrane in wild-type HSV-1(F)-infected cells, in agreement with the immunofluorescence results described above (Fig. 10, 13, 14 and 15). p32 was also found in areas in the nucleus with many capsids and on a significant fraction of capsids in the nucleus (Fig. 23B and Fig. 24A).

In contrast, p32 was detected to a much lesser extent in areas in the nucleus without capsids (Fig. 24A). These results suggested that p32 was specifically recruited to capsids in the nucleus in wild-type HSV-1(F) infected cells. In addition, p32 was detected on most primary enveloped virions in the perinuclear space (Fig. 23C and D) and on capsids in the cytoplasm (Fig. 23E and Fig. 24B), but was barely detected on secondary enveloped cytoplasmic and extracellular virions (Fig. 23F and G, and Fig. 24B and C). In agreement with these results, p32 was not detected on purified extracellular virions by immunoblotting, whereas it was detected on purified cell-associated virions, which consisted of nucleocapsids, primary enveloped virions and secondary enveloped virions (Fig. 25). These results suggested that p32 was a component of primary enveloped virions and that HSV-1 virions acquired p32 in the nucleus prior to primary envelopment and subsequently lost p32 during secondary envelopment.

Next, we attempted to localize UL47 in HSV-1-infected cells at the ultra-structural level. Preliminary experiments indicated that the anti-UL47 antibody generated in this study was not useful for immunoelectron microscopy (data not shown). Therefore, we attempted to detect tagged UL47 in Vero cells infected with

YK524 (mRFP1-UL47) or YK536 (MEF-UL47) using various rabbit polyclonal and mouse monoclonal antibodies to the mRFP1, Flag and Myc tags. Among the antibodies tested, only anti-Myc mouse monoclonal antibody bound significantly to Vero cells infected with YK536 (MEF-UL47) (Fig. 26 and Fig. 27), but not to wild-type HSV-1(F)-infected Vero cells (data not shown). MEF-tagged UL47 was detected throughout the nucleus (Fig. 27A) and at the nuclear membrane (Fig. 26A) by immunoelectron microscopy of YK536 (MEF-UL47)-infected Vero cells, in agreement with the localization of mRFP1-UL47 by fluorescence microscopy (Fig. 13 and 15). We noted that MEF-tagged UL47 was detected on nuclear capsids (Fig. 26A and B and Fig. 27A) but, unlike p32 as described above (Fig. 24A), the density of immunostained MEF-tagged UL47 in nuclear domains with capsid aggregates was approximately the same as in domains without capsids (Fig. 27A). These observations raised the possibility that MEF-UL47 was not specifically associated with nuclear capsids. MEF-tagged UL47 was also detected on most primary enveloped virions in the perinuclear space, secondary enveloped virions in the cytoplasm and extracellular virions (Fig. 26 C to G and Fig. 27B and C), suggesting that UL47 was a component of both primary and secondary enveloped virions.

Discussion

Tandem affinity purification of transiently expressed HSV-1 UL47 in Vero cells coupled with mass spectrometry-based proteomics technology identified a potential interaction between UL47 and cellular protein p32, which was verified by reciprocal co-immunoprecipitation studies in cells transiently overexpressing MEF-tagged UL47 and/or Flag-tagged p32. We confirmed the interaction of UL47 with p32 in HSV-1-infected cells: p32 co-precipitated with MEF-tagged UL47 in lysates of cells infected with recombinant virus YK536 (MEF-UL47) and, in reciprocal experiments, UL47 co-precipitated with MEF-tagged p32 in lysates of cells infected with recombinant virus YK537 (MEF-p32). Subsequent studies showed that knock-down of p32 significantly reduced HSV-1 replication in the presence of UL47, but the effect of p32 knock-down on viral replication was considerably attenuated in the absence of UL47. In reciprocal experiments, the effect of the UL47-null mutation on HSV-1 replication was reduced in p32 knock-down cells. These results indicated that p32 played a significant role in HSV-1 replication, and that UL47 and p32 regulated the same HSV-1 replication pathway.

In agreement with previous reports that HVS and HSV-1 infections caused

translocation of p32 from the cytoplasm to the nucleus and/or nuclear rim (Bryant et al., 2000; Hall et al., 2002), this study showed that p32 redistributed from the cytoplasm to the nuclear membrane in wild-type HSV-1 infected Vero cells. In contrast, p32 was predominantly localized in the cytoplasm of Vero cells that were mock-infected or infected with the UL47-null mutant virus (YK545). These results indicated that UL47 was required for proper localization of p32 at the nuclear membrane in HSV-1-infected cells and suggested that the interaction between p32 and UL47 in HSV-1-infected cells was significant for their roles in viral nuclear egress. These features of p32 and UL47 are in agreement with previous reports that UL47 regulates the subcellular localization of Us3, an HSV-1 kinase that interacts with UL47 in infected cells (Kato et al., 2011), and that many herpesvirus proteins that interact with p32, including HSV-1 ICP27, EBV EBNA-1, HVS ORF63 and MHV-68 M2, can cause the redistribution of p32 when these viral proteins are transiently overexpressed (Bryant et al., 2000; Hall et al., 2002; Liang et al., 2004; Van Scoy et al., 2000). However, the roles of these herpesvirus proteins in regulating p32 localization in the context of viral infection remain to be determined. In addition, We noted that p32 appeared to be distributed more diffusely in the cytoplasm of cells infected with

YK545 (ΔUL47) than in mock-infected cells. It has been reported that viruses regulated mitochondrial membrane potential in host cells, destroyed mitochondrial membrane permeabilization and induced the release of apoptotic protein from mitochondrial (Galluzzi et al., 2008; Sanjeew and T, 2013). The difference in distribution raised the possibility that p32 was released from the mitochondrial in HSV-1-infected cells and still localized in the cytoplasm in the absence of UL47.

In this study, we found that MEF-tagged UL47 co-immunoprecipitated with UL34, UL31, Us3 and p32; MEF-tagged UL31 co-immunoprecipitated with UL34, Us3, UL47 and p32; and MEF-tagged UL34 co-immunoprecipitated with UL31, UL47, Us3 and p32. Based on these data and the immunoelectron microscopy results in this and previous studies showing that p32, UL47, UL31, UL34 and Us3 are components of primary enveloped virions, it seemed possible that co-immunoprecipitation of UL31, UL34, UL47, Us3 and p32 indicated that these viral and cellular proteins may associate in intact capsids. However, since we found that all of these MEF-tagged viral proteins did not co-immunoprecipitate with herpesvirus capsid protein VP23, this possibility seemed less likely. Taken together, these results indicated that UL47 formed a complex with UL34, UL31, Us3 and/or p32, and that p32 formed a complex

with UL34, UL31 and/or UL47 in HSV-1-infected cells. This conclusion was in agreement with previous reports (Kato et al., 2011; Scholtes et al., 2010; Yang and Baines, 2011) that, in HSV-1-infected cells, UL47 interacted with viral capsid protein UL17, which further formed a complex with UL31 and viral capsid protein UL25, and that UL47 interacted with Us3. At present it remains to be determined whether UL31, UL34, UL47, Us3 and p32 form a high-order complex or whether the interactions among these viral proteins and p32 are temporary and occur in a sequential order in HSV-1-infected cells. However, the reciprocal co-immunoprecipitation experiments in this and previous studies (Kato et al., 2011; Reynolds et al., 2001) showing co-immunoprecipitation of Us3 and UL47 and of UL31 and UL34 suggested that these interactions form a high-order complex of UL31, UL34, UL47, Us3 and p32 in infected cells. In particular, UL31 and UL34 have been shown to be predominantly detected at the nuclear membrane in wild-type HSV-1-infected cells by immunofluorescence microscopy (Reynolds et al., 2001). Therefore, it is likely that the interactions of UL31 and UL34 with UL47, Us3 and p32 observed in this study occurred mainly at the nuclear membrane in HSV-1-infected cells. Furthermore, we showed here that, in the absence of Us3 kinase activity, UL34, UL31, UL47 and p32

were all aberrantly localized and co-localized in punctate structures at the nuclear membrane. This result suggested that localization of UL31, UL34, UL47 and p32 at the nuclear membrane were all regulated by Us3 kinase activity and supported the hypothesis that these viral proteins, p32, and probably Us3 formed a complex at the nuclear membrane in HSV-1-infected cells. We showed that UL47 formed a complex with p32 in infected cells and further co-localized with p32 at the nuclear membrane. It has been reported that p32 could interact with Lamin B receptor (Simos and Georgatos, 1994). Accordingly, there was the possibility that UL47 localized at the nuclear membrane dependently on p32. Since we showed that UL47, UL 31, UL34, Us3 and p32 formed a high order complex at nuclear membrane and it has been reported that UL34 was a type 2 membrane protein and localized in nuclear membrane(Bjerke and Roller, 2006). Taken together, this possibility seemed very low.

Quantitative electron microscopic analysis of infected Vero and HEp-2 cells showed that, in the absence of UL47, primary enveloped virions in the perinuclear space were barely detectable and the prevalence of this type of virion was substantially reduced. In contrast, the frequency of nuclear capsids increased. The accumulation of nuclear capsids and the lack of primary enveloped virions in the perinuclear space in

the absence of UL47 likely reflected an imbalance between the rate of virion delivery into the perinuclear space and the rate of egress from this region. Thus, it appeared that the rate of viral egress from the nucleoplasm decreased in the absence of UL47 compared to that in the presence of UL47, but the rate of egress from the perinuclear space in the absence of UL47 was similar to that in the presence of UL47. Based on these results, UL47 appeared to be required for efficient primary envelopment of nucleocapsids in HSV-1 nuclear egress. In support of this hypothesis, we showed that UL47 was detected at the inner nuclear membrane by immunoelectron microscopy. It has been reported that, in cells infected with a UL34- or UL31-null mutant HSV-1, no enveloped virions were detected in the perinuclear space, cytoplasm, or at the cell surface (Chang et al., 1997; Roller et al., 2000), indicating that UL31 and UL34 functions were required for primary envelopment of nucleocapsids. In this study, primary enveloped virions in the perinuclear space were barely detected in cells infected with the UL47-null mutant HSV-1, as was observed in cells infected with the UL31- or UL34-null mutant HSV-1, but the prevalence of enveloped virions in the cytoplasm of cells infected with the UL47-null mutant HSV-1, although detectable, was decreased. These observations suggested that UL47 was not as essential for

primary envelopment of nucleocapsids at the nuclear membrane as UL34 and UL31, but played a regulatory role in this process. UL47 may regulate the optimal primary envelopment activity of the UL34/UL31 complex by interaction with the complex. This hypothesis was supported by the observation in this study that UL47 interacted with UL31 and UL34 in infected cells and that UL47 was a component of primary enveloped virions, which enabled UL47 to interact with the UL34/UL31 complex during primary envelopment. As described above, UL47 was reported to form a complex with UL17, a component of the HSV-1 CVSC, and, therefore, may interact with UL31 to recruit HSV nucleocapsids for primary envelopment (Toropova et al., 2011; Yang and Baines, 2011). In addition, we showed here that UL47 formed a complex with VP5, a major HSV-1 capsid protein. Therefore, UL47 may up-regulate the primary envelopment of nucleocapsids by promoting recruitment of nucleocapsids through interaction with the UL17/UL25/UL31 complex and with VP5, which may further stabilize the association of capsids with the UL34/UL31 complex at the nuclear membrane.

Electron microscopic analysis of HSV-1-infected sh-p32-HEp-2 and sh-Luc-HEp-2 cells showed that p32 knock-down significantly induced membranous

invagination structures containing several primary enveloped virions adjacent to the nuclear membrane. Immunofluorescence analysis of these infected cells also showed that p32 knock-down resulted in aberrant localization of UL31 and UL34 in punctate structures adjacent to the nuclear membrane, which protruded into the nucleoplasm and may correspond to the invaginations at the nuclear membrane detected by electron microscopy. The membranous invaginations have also been reported to be induced by mutation(s) that block Us3 kinase activity, expression of both gB and gH, Us3 phosphorylation of UL31, and Us3 phosphorylation of gB together with expression of gH (Farnsworth et al., 2007; Kato et al., 2009; Mou et al., 2009; Ryckman and Roller, 2004; Wisner et al., 2009). Aberrant virion accumulation in membranous invagination structures has been suggested to be the result of a reduction in the rate of virion egress from the perinuclear space, while the rate of egress from the nucleoplasm was unchanged. This led to the hypothesis that Us3 kinase activity, the presence of gB in combination with gH/gL, and Us3 phosphorylation of UL31 and gB were all required for efficient virion de-envelopment in HSV-1 nuclear egress. In this model, p32 was suggested to regulate de-envelopment during HSV-1 nuclear egress. p32 may be involved in perinuclear fusion during HSV-1 de-envelopment by regulating the

fusogenic activity of gB, and/or Us3 phosphorylation of UL31 and gB. In support of this hypothesis, we have shown here that p32 was a component of primary enveloped virions, which would enable p32 to interact with Us3, gB, gH/gL and UL31, all of which were reported to be components of primary enveloped virions (Farnsworth et al., 2007; Reynolds et al., 2002) during HSV-1 de-envelopment. Furthermore, it has been reported that p32 binds to arginine-rich regions of its target proteins (Hall et al., 2002). Interestingly, the consensus target sequence of Us3 is the arginine-rich sequence RnX(S/T)YY, where n is ≥ 2, X can be Arg, Ala, Val, Pro, or Ser, and Y can be any amino acid except an acidic residue (Leader, 1993; Leader et al., 1991; Purves et al., 1986). Therefore, p32 may bind to the phosphorylation site of Us3 substrates and somehow regulate Us3 phosphorylation of its substrate(s), such as UL31 and gB, to promote perinuclear fusion activity for HSV-1 de-envelopment.

We noted that the invagination structures containing primary enveloped virions and the punctate structures of the UL34/UL31 complex induced by p32 knock-down were not observed in the absence of UL47, although p32 knock-down had no effect on the reduction in primary enveloped virions in the perinuclear space or accumulation of capsids in the nucleus induced by the UL47-null mutation. These

observations indicated that UL47 acted in the HSV-1 nuclear egress pathway before the de-envelopment step in which p32 was suggested to be involved, and supported our hypotheses above that UL47 played a role in primary envelopment and that UL47 and p32 regulated HSV-1 replication in the same pathway. In addition, p32 redistribution to the nuclear membrane mediated by UL47 and/or the interaction of p32 with UL47 may be necessary for p32 to function in de-envelopment at the nuclear membrane.

It has been reported that p32 interacted with the components of the HCMV NEC, UL50 (a homolog of HSV-1 UL34) and UL53 (a homolog of HSV-1 31), and with HCMV protein kinase UL97 (a homolog of HSV-1 UL13), lamin B receptor (LBR) and protein kinase C (PKC) (Marschall et al., 2005; Milbradt et al., 2009; Robles-Flores et al., 2002; Simos and Georgatos, 1994). Although a direct role of p32 in HCMV nuclear egress has not been determined, these observations raised the interesting possibility that p32 may play a conserved role in the nuclear egress of alpha- and betaherpesviruses. This may also be the case in gammaherpesviruses, based on the observations that infection of cells with gammaherpesviruses, HVS and murid herpesvirus 68 (MHV68) translocated p32 to the nuclear membrane (Hall et al., 2002; Liang et al., 2004), as was observed with HSV-1 infection in this study. In

addition, HSV-1 Us3 and HCMV UL97 have been shown to phosphorylate p32 in vitro in this and previous studies (Marschall et al., 2005), suggesting that phosphorylation of p32 mediated by herpesvirus protein kinases was involved in regulation of p32 activity in viral nuclear egress. In agreement with this suggestion, we have shown here that p32 knock-down induced membranous invaginations containing primary enveloped virions, which also has been observed in cells infected with HSV-1 Us3 kinase-dead mutant viruses (Ryckman and Roller, 2004). Furthermore, HCMV UL97 and Epstein-Barr virus (EBV) BGLF4 (a homolog of HCMV UL97) were reported to be critical for viral nuclear egress (Gershburg et al., 2007; Krosky et al., 2003), although it remains to be determined whether EBV BGLF4 phosphorylates p32. Since UL47 is only conserved in alphaherpesviruses, the factors regulating herpesvirus nuclear egress may vary among alpha-, beta- and gammaherpesviruses, although these factors may include the cellular protein p32 and a protein kinase to phosphorylate p32, such as the HSV-1 Us3 homologues in alphaherpesviruses and HCMV UL97 homologues in betaherpesviruses, in addition to the conserved core proteins of NECs.

Our immunoelectron microscopy data showing that HSV-1 UL47 was a component of both primary enveloped virions and extracellular virions was not in

agreement with previous reports by Naldinho-Souto et al. (Naldinho-Souto et al., 2006) that HSV-1 UL47 tagged with yellow fluorescent protein (YFP) was not detected in primary enveloped virions by immunoelectron microscopy, but was detected in extracellular virions. A similar observation was also obtained with VP22 tagged with green fluorescent protein (GFP) (Naldinho-Souto et al., 2006). However, biochemical isolation and characterization of wild-type HSV-1 primary enveloped virions by Padula et al. (Padula et al., 2009) showed that untagged VP22 was detected as a component of primary enveloped virions. Therefore, it may be more difficult to detect a fluorescent-tagged protein component of primary enveloped virions by immunoelectron microscopy than to detect it in extracellular virions. Since Bilali et al. (El Bilali et al., 2013) recently reported that tagging tegument proteins with a fluorescent protein had a significant effect on incorporation of the tagged proteins into virions, UL47 tagged with a fluorescent protein may be incorporated into primary enveloped virions much less efficiently than untagged UL47 or UL47 tagged with MEF, which is much smaller than the fluorescent proteins. Our data also were not in agreement with the previous report that pseudorabies virus (PRV) UL47 was not present in primary enveloped virions (Granzow et al., 2004). It appears that, despite

their genetic similarities, HSV-1 and PRV differ in the composition of their virions, since HSV-1 primary enveloped virions contain gB, gD, gH/gL, gM, VP22, VHS, VP16 and UL11, but PRV does not (Baines et al., 1995; Baines et al., 2007; Farnsworth et al., 2007; Mettenleiter et al., 2013; Naldinho-Souto et al., 2006; Padula et al., 2009; Read and Patterson, 2007; Stannard et al., 1996). Alternatively, UL47 may have been present in PRV primary enveloped virions, but could not be detected with the antibody used in that study.

In conclusion, the data presented here begin to elucidate the interaction of HSV-1 protein UL47 and host cell protein p32 in regulating viral nuclear egress. The vesicle-mediated viral nuclear egress process may be a general model for transport of large macromolecular complexes from the nucleus to the cytoplasm, and may involve viral and cellular proteins other than those reported to date. Further studies to identify other novel viral and cellular proteins that regulate the vesicle-mediated viral egress process and to elucidate the mechanisms of these regulatory proteins, including UL47 and p32, in this process will be needed and are currently underway in this laboratory.

References

Ann M. A, and Don, G. (2013). Varicella-Zoster Virus, p. 2015-2057. in Knipe D M , Howley P M, et al, Fields virology, 6th ed,vol 2 Lippincott Williams & Wilkins, Philadelphia, PA.

Arii, J., Goto, H., Suenaga, T., Oyama, M., Kozuka-Hata, H., Imai, T., Minowa, A., Akashi, H., Arase, H., Kawaoka, Y., and Kawaguchi, Y. (2010). Non-muscle myosin IIA is a functional entry receptor for herpes simplex virus-1. Nature *467*, 859-862.

Baines, J. D. (2011). Herpes simplex virus capsid assembly and DNA packaging: a present and future antiviral drug target. Trends Microbiol *19*, 606-613.

Baines, J. D., Jacob, R. J., Simmerman, L., and Roizman, B. (1995). The herpes simplex virus 1 UL11 proteins are associated with cytoplasmic and nuclear membranes and with nuclear bodies of infected cells. J Virol *69*, 825-833.

Baines, J. D., Wills, E., Jacob, R. J., Pennington, J., and Roizman, B. (2007). Glycoprotein M of herpes simplex virus 1 is incorporated into virions during budding at the inner nuclear membrane. J Virol *81*, 800-812.

Batterson, W., Furlong, D., and Roizman, B. (1983). Molecular genetics of herpes

simplex virus. VIII. further characterization of a temperature-sensitive mutant defective in release of viral DNA and in other stages of the viral reproductive cycle. J Virol *45*, 397-407.

Beatch, M. D., Everitt, J. C., Law, L. J., and Hobman, T. C. (2005). Interactions between rubella virus capsid and host protein p32 are important for virus replication. J Virol *79*, 10807-10820.

Bernard, R., David M, K., and W., R. J. (2013). Herpes Simplex Viruses, p. 1823-1825. in Knipe D M , Howley P M, et al (ed), Fields virology, 6th ed,vol 2 Lippincott Williams & Wilkins, Philadelphia, PA.

Berro, R., Kehn, K., de la Fuente, C., Pumfery, A., Adair, R., Wade, J., Colberg-Poley, A. M., Hiscott, J., and Kashanchi, F. (2006). Acetylated Tat regulates human immunodeficiency virus type 1 splicing through its interaction with the splicing regulator p32. J Virol *80*, 3189-3204.

Bjerke, S. L., and Roller, R. J. (2006). Roles for herpes simplex virus type 1 UL34 and US3 proteins in disrupting the nuclear lamina during herpes simplex virus type 1 egress. Virology *347*, 261-276.

Blossom A. D, and C., E. (2013). Kaposi' A. Sarcoma-Associated Herpesvirus.

p.2080-2128. in Knipe D M , Howley P M, et al, Fields virology, 6th ed,vol 2 Lippincott Williams & Wilkins, Philadelphia, PA.

Brokstad, K. A., Kalland, K. H., Russell, W. C., and Matthews, D. A. (2001). Mitochondrial protein p32 can accumulate in the nucleus. Biochem Biophys Res Commun *281*, 1161-1169.

Bruni, R., and Roizman, B. (1996). Open reading frame P--a herpes simplex virus gene repressed during productive infection encodes a protein that binds a splicing factor and reduces synthesis of viral proteins made from spliced mRNA. Proc Natl Acad Sci U S A *93*, 10423-10427.

Bryant, H. E., Matthews, D. A., Wadd, S., Scott, J. E., Kean, J., Graham, S., Russell, W. C., and Clements, J. B. (2000). Interaction between herpes simplex virus type 1 IE63 protein and cellular protein p32. J Virol *74*, 11322-11328.

Chang, Y. E., Van Sant, C., Krug, P. W., Sears, A. E., and Roizman, B. (1997). The null mutant of the U(L)31 gene of herpes simplex virus 1: construction and phenotype in infected cells. J Virol *71*, 8307-8315.

Desai, P. J., Pryce, E. N., Henson, B. W., Luitweiler, E. M., and Cothran, J. (2012). Reconstitution of the Kaposi's sarcoma-associated herpesvirus nuclear egress

complex and formation of nuclear membrane vesicles by coexpression of ORF67 and ORF69 gene products. J Virol *86*, 594-598.

Dobrikova, E., Shveygert, M., Walters, R., and Gromeier, M. (2010). Herpes simplex virus proteins ICP27 and UL47 associate with polyadenylate-binding protein and control its subcellular distribution. J Virol *84*, 270-279.

Donnelly, M., and Elliott, G. (2001). Nuclear localization and shuttling of herpes simplex virus tegument protein VP13/14. J Virol *75*, 2566-2574.

Donnelly, M., Verhagen, J., and Elliott, G. (2007). RNA binding by the herpes simplex virus type 1 nucleocytoplasmic shuttling protein UL47 is mediated by an N-terminal arginine-rich domain that also functions as its nuclear localization signal. J Virol *81*, 2283-2296.

Edward S. M, Jr. Thomas. S, Paul D. G, and P, R. F. (2013). Cytomegaloviruses, p. 1960-2014. in Knipe D M , Howley P M, et al, Fields virology, 6th ed,vol 2 Lippincott Williams & Wilkins, Philadelphia, PA.

El Bilali, N., Radtke, K., and Lippe, R. (2013). Analysis of the HSV-1 Tegument by Flow cytometry, abstr 4.07, p 100. Abstr 38th Annual International Herpesvirus Workshop, Grand Rapids, Michigan, USA.

Farnsworth, A., Wisner, T. W., Webb, M., Roller, R., Cohen, G., Eisenberg, R., and Johnson, D. C. (2007). Herpes simplex virus glycoproteins gB and gH function in fusion between the virion envelope and the outer nuclear membrane. Proc Natl Acad Sci U S A *104*, 10187-10192.

Galluzzi, L., Brenner, C., Morselli, E., Touat, Z., and Kroemer, G. (2008). Viral control of mitochondrial apoptosis. PLoS Pathog *4*, e1000018.

Gershburg, E., Raffa, S., Torrisi, M. R., and Pagano, J. S. (2007). Epstein-Barr virus-encoded protein kinase (BGLF4) is involved in production of infectious virus. J Virol *81*, 5407-5412.

Granzow, H., Klupp, B. G., and Mettenleiter, T. C. (2004). The pseudorabies virus US3 protein is a component of primary and of mature virions. J Virol *78*, 1314-1323.

Hall, K. T., Giles, M. S., Calderwood, M. A., Goodwin, D. J., Matthews, D. A., and Whitehouse, A. (2002). The Herpesvirus Saimiri open reading frame 73 gene product interacts with the cellular protein p32. J Virol *76*, 11612-11622.

Itahana, K., and Zhang, Y. (2008). Mitochondrial p32 is a critical mediator of ARF-induced apoptosis. Cancer Cell *13*, 542-553.

Johnson, D. C., and Baines, J. D. (2011). Herpesviruses remodel host membranes for

virus egress. Nat Rev Microbiol *9*, 382-394.

Johnson, K. M., Mahajan, S. S., and Wilson, A. C. (1999). Herpes simplex virus transactivator VP16 discriminates between HCF-1 and a novel family member, HCF-2. J Virol *73*, 3930-3940.

Kato, A., Arii, J., Shiratori, I., Akashi, H., Arase, H., and Kawaguchi, Y. (2009). Herpes simplex virus 1 protein kinase Us3 phosphorylates viral envelope glycoprotein B and regulates its expression on the cell surface. J Virol *83*, 250-261.

Kato, A., Hirohata, Y., Arii, J., and Kawaguchi, Y. (2014). Phosphorylation of herpes simplex virus 1 dUTPase upregulated viral dUTPase activity to compensate for low cellular dUTPase activity for efficient viral replication. J Virol *88*, 7776-7785.

Kato, A., Liu, Z., Minowa, A., Imai, T., Tanaka, M., Sugimoto, K., Nishiyama, Y., Arii, J., and Kawaguchi, Y. (2011). Herpes simplex virus 1 protein kinase Us3 and major tegument protein UL47 reciprocally regulate their subcellular localization in infected cells. J Virol *85*, 9599-9613.

Kato, A., Tanaka, M., Yamamoto, M., Asai, R., Sata, T., Nishiyama, Y., and Kawaguchi, Y. (2008). Identification of a physiological phosphorylation site of the herpes

simplex virus 1-encoded protein kinase Us3 which regulates its optimal catalytic activity in vitro and influences its function in infected cells. J Virol *82*, 6172-6189.

Kato, A., Yamamoto, M., Ohno, T., Kodaira, H., Nishiyama, Y., and Kawaguchi, Y. (2005). Identification of proteins phosphorylated directly by the Us3 protein kinase encoded by herpes simplex virus 1. J Virol *79*, 9325-9331.

Kawaguchi, Y., Van Sant, C., and Roizman, B. (1997). Herpes simplex virus 1 alpha regulatory protein ICP0 interacts with and stabilizes the cell cycle regulator cyclin D3. J Virol *71*, 7328-7336.

Kittlesen, D. J., Chianese-Bullock, K. A., Yao, Z. Q., Braciale, T. J., and Hahn, Y. S. (2000). Interaction between complement receptor gC1qR and hepatitis C virus core protein inhibits T-lymphocyte proliferation. J Clin Invest *106*, 1239-1249.

Klupp, B. G., Granzow, H., Fuchs, W., Keil, G. M., Finke, S., and Mettenleiter, T. C. (2007). Vesicle formation from the nuclear membrane is induced by coexpression of two conserved herpesvirus proteins. Proc Natl Acad Sci U S A *104*, 7241-7246.

Knipe, D. M., and Cliffe, A. (2008). Chromatin control of herpes simplex virus lytic and latent infection. Nat Rev Microbiol *6*, 211-221.

Koichi. Y, Yasuko. M, and P., P. E. (2013). Human Herpesviruses 6 and 7, p. 2058-2079. in Knipe D M , Howley P M, et al, Fields virology, 6th ed,vol 2 Lippincott Williams & Wilkins, Philadelphia, PA.

Kramer, T., and Enquist, L. W. (2013). Directional spread of alphaherpesviruses in the nervous system. Viruses *5*, 678-707.

Krosky, P. M., Baek, M. C., and Coen, D. M. (2003). The human cytomegalovirus UL97 protein kinase, an antiviral drug target, is required at the stage of nuclear egress. J Virol *77*, 905-914.

Kwong, A. D., and Frenkel, N. (1989). The herpes simplex virus virion host shutoff function. J Virol *63*, 4834-4839.

Leader, D. P. (1993). Viral protein kinases and protein phosphatases. Pharmacol Ther *59*, 343-389.

Leader, D. P., Deana, A. D., Marchiori, F., Purves, F. C., and Pinna, L. A. (1991). Further definition of the substrate specificity of the alpha-herpesvirus protein kinase and comparison with protein kinases A and C. Biochim Biophys Acta *1091*, 426-431.

Liang, X., Shin, Y. C., Means, R. E., and Jung, J. U. (2004). Inhibition of

interferon-mediated antiviral activity by murine gammaherpesvirus 68 latency-associated M2 protein. J Virol *78*, 12416-12427.

Lim, B. L., White, R. A., Hummel, G. S., Schwaeble, W., Lynch, N. J., Peerschke, E. I., Reid, K. B., and Ghebrehiwet, B. (1998). Characterization of the murine gene of gC1qBP, a novel cell protein that binds the globular heads of C1q, vitronectin, high molecular weight kininogen and factor XII. Gene *209*, 229-237.

Loret, S., Guay, G., and Lippe, R. (2008). Comprehensive characterization of extracellular herpes simplex virus type 1 virions. J Virol *82*, 8605-8618.

Lu, P. D., Galanakis, D. K., Ghebrehiwet, B., and Peerschke, E. I. (1999). The receptor for the globular "heads" of C1q, gC1q-R, binds to fibrinogen/fibrin and impairs its polymerization. Clin Immunol *90*, 360-367.

Luo, Y., Yu, H., and Peterlin, B. M. (1994). Cellular protein modulates effects of human immunodeficiency virus type 1 Rev. J Virol *68*, 3850-3856.

Maric, M., Shao, J., Ryan, R. J., Wong, C. S., Gonzalez-Alegre, P., and Roller, R. J. (2011). A functional role for TorsinA in herpes simplex virus 1 nuclear egress. J Virol *85*, 9667-9679.

Marschall, M., Marzi, A., aus dem Siepen, P., Jochmann, R., Kalmer, M., Auerochs, S.,

Lischka, P., Leis, M., and Stamminger, T. (2005). Cellular p32 recruits cytomegalovirus kinase pUL97 to redistribute the nuclear lamina. J Biol Chem *280*, 33357-33367.

Maruzuru, Y., Fujii, H., Oyama, M., Kozuka-Hata, H., Kato, A., and Kawaguchi, Y. (2013). Roles of p53 in herpes simplex virus 1 replication. J Virol *87*, 9323-9332.

Matthews, D. A., and Russell, W. C. (1998). Adenovirus core protein V interacts with p32--a protein which is associated with both the mitochondria and the nucleus. J Gen Virol *79 (Pt 7)*, 1677-1685.

Mettenleiter, T. C., Muller, F., Granzow, H., and Klupp, B. G. (2013). The way out: what we know and do not know about herpesvirus nuclear egress. Cell Microbiol *15*, 170-178.

Milbradt, J., Auerochs, S., Sticht, H., and Marschall, M. (2009). Cytomegaloviral proteins that associate with the nuclear lamina: components of a postulated nuclear egress complex. J Gen Virol *90*, 579-590.

Morimoto, T., Arii, J., Tanaka, M., Sata, T., Akashi, H., Yamada, M., Nishiyama, Y., Uema, M., and Kawaguchi, Y. (2009). Differences in the regulatory and functional effects of the Us3 protein kinase activities of herpes simplex virus 1 and 2. J Virol

83, 11624-11634.

Mossman, K. L., Sherburne, R., Lavery, C., Duncan, J., and Smiley, J. R. (2000). Evidence that herpes simplex virus VP16 is required for viral egress downstream of the initial envelopment event. J Virol *74*, 6287-6299.

Mou, F., Forest, T., and Baines, J. D. (2007). US3 of herpes simplex virus type 1 encodes a promiscuous protein kinase that phosphorylates and alters localization of lamin A/C in infected cells. J Virol *81*, 6459-6470.

Mou, F., Wills, E., and Baines, J. D. (2009). Phosphorylation of the U(L)31 protein of herpes simplex virus 1 by the U(S)3-encoded kinase regulates localization of the nuclear envelopment complex and egress of nucleocapsids. J Virol *83*, 5181-5191.

Mou, F., Wills, E. G., Park, R., and Baines, J. D. (2008). Effects of lamin A/C, lamin B1, and viral US3 kinase activity on viral infectivity, virion egress, and the targeting of herpes simplex virus U(L)34-encoded protein to the inner nuclear membrane. J Virol *82*, 8094-8104.

Naldinho-Souto, R., Browne, H., and Minson, T. (2006). Herpes simplex virus tegument protein VP16 is a component of primary enveloped virions. J Virol *80*, 2582-2584.

Noda, T., Sagara, H., Yen, A., Takada, A., Kida, H., Cheng, R. H., and Kawaoka, Y. (2006). Architecture of ribonucleoprotein complexes in influenza A virus particles. Nature *439*, 490-492.

Noda, T., Sugita, Y., Aoyama, K., Hirase, A., Kawakami, E., Miyazawa, A., Sagara, H., and Kawaoka, Y. (2012). Three-dimensional analysis of ribonucleoprotein complexes in influenza A virus. Nat Commun *3*, 639.

Nozawa, N., Kawaguchi, Y., Tanaka, M., Kato, A., Kato, A., Kimura, H., and Nishiyama, Y. (2005). Herpes simplex virus type 1 UL51 protein is involved in maturation and egress of virus particles. J Virol *79*, 6947-6956.

Padula, M. E., Sydnor, M. L., and Wilson, D. W. (2009). Isolation and preliminary characterization of herpes simplex virus 1 primary enveloped virions from the perinuclear space. J Virol *83*, 4757-4765.

Park, R., and Baines, J. D. (2006). Herpes simplex virus type 1 infection induces activation and recruitment of protein kinase C to the nuclear membrane and increased phosphorylation of lamin B. J Virol *80*, 494-504.

Philip E, P., and Bernard, R. (2013). Herpesviridae, p. 1802-1822. in Knipe D M , Howley P M, et al, Fields virology, 6th ed,vol 2 Lippincott Williams & Wilkins,

Philadelphia, PA.

Purves, F. C., Deana, A. D., Marchiori, F., Leader, D. P., and Pinna, L. A. (1986). The substrate specificity of the protein kinase induced in cells infected with herpesviruses: studies with synthetic substrates [corrected] indicate structural requirements distinct from other protein kinases. Biochim Biophys Acta *889*, 208-215.

Purves, F. C., Spector, D., and Roizman, B. (1991). The herpes simplex virus 1 protein kinase encoded by the US3 gene mediates posttranslational modification of the phosphoprotein encoded by the UL34 gene. J Virol *65*, 5757-5764.

Read, G. S., and Patterson, M. (2007). Packaging of the virion host shutoff (Vhs) protein of herpes simplex virus: two forms of the Vhs polypeptide are associated with intranuclear B and C capsids, but only one is associated with enveloped virions. J Virol *81*, 1148-1161.

Reynolds, A. E., Liang, L., and Baines, J. D. (2004). Conformational changes in the nuclear lamina induced by herpes simplex virus type 1 require genes U(L)31 and U(L)34. J Virol *78*, 5564-5575.

Reynolds, A. E., Ryckman, B. J., Baines, J. D., Zhou, Y., Liang, L., and Roller, R. J.

(2001). U(L)31 and U(L)34 proteins of herpes simplex virus type 1 form a complex that accumulates at the nuclear rim and is required for envelopment of nucleocapsids. J Virol *75*, 8803-8817.

Reynolds, A. E., Wills, E. G., Roller, R. J., Ryckman, B. J., and Baines, J. D. (2002). Ultrastructural localization of the herpes simplex virus type 1 UL31, UL34, and US3 proteins suggests specific roles in primary envelopment and egress of nucleocapsids. J Virol *76*, 8939-8952.

Richard M, L., Elliott, K., and Jeffrey I, C. (2013). Epstein-Barr Virus, p. 1898-1959. in Knipe D M , Howley P M, et al, Fields virology, 6th ed,vol 2 Lippincott Williams & Wilkins, Philadelphia, PA.

Robles-Flores, M., Rendon-Huerta, E., Gonzalez-Aguilar, H., Mendoza-Hernandez, G., Islas, S., Mendoza, V., Ponce-Castaneda, M. V., Gonzalez-Mariscal, L., and Lopez-Casillas, F. (2002). p32 (gC1qBP) is a general protein kinase C (PKC)-binding protein; interaction and cellular localization of P32-PKC complexes in ray hepatocytes. J Biol Chem *277*, 5247-5255.

Roller, R. J., Zhou, Y., Schnetzer, R., Ferguson, J., and DeSalvo, D. (2000). Herpes simplex virus type 1 U(L)34 gene product is required for viral envelopment. J

Virol *74*, 117-129.

Rubinstein, D. B., Stortchevoi, A., Boosalis, M., Ashfaq, R., Ghebrehiwet, B., Peerschke, E. I., Calvo, F., and Guillaume, T. (2004). Receptor for the globular heads of C1q (gC1q-R, p33, hyaluronan-binding protein) is preferentially expressed by adenocarcinoma cells. Int J Cancer *110*, 741-750.

Ryckman, B. J., and Roller, R. J. (2004). Herpes simplex virus type 1 primary envelopment: UL34 protein modification and the US3-UL34 catalytic relationship. J Virol *78*, 399-412.

Sanjeew, K. A., and T, S. K. (2013). Viruses as Modeulators of Mitochondrial Functions. Advances in Virology *738794*, 1-17.

Scholtes, L. D., Yang, K., Li, L. X., and Baines, J. D. (2010). The capsid protein encoded by U(L)17 of herpes simplex virus 1 interacts with tegument protein VP13/14. J Virol *84*, 7642-7650.

Shu, M., Taddeo, B., Zhang, W., and Roizman, B. (2013). Selective degradation of mRNAs by the HSV host shutoff RNase is regulated by the UL47 tegument protein. Proc Natl Acad Sci U S A *110*, E1669-1675.

Simos, G., and Georgatos, S. D. (1994). The lamin B receptor-associated protein p34

shares sequence homology and antigenic determinants with the splicing factor 2-associated protein p32. FEBS Lett *346*, 225-228.

Speese, S. D., Ashley, J., Jokhi, V., Nunnari, J., Barria, R., Li, Y., Ataman, B., Koon, A., Chang, Y. T., Li, Q., *et al.* (2012). Nuclear envelope budding enables large ribonucleoprotein particle export during synaptic Wnt signaling. Cell *149*, 832-846.

Stannard, L. M., Himmelhoch, S., and Wynchank, S. (1996). Intra-nuclear localization of two envelope proteins, gB and gD, of herpes simplex virus. Arch Virol *141*, 505-524.

Sugimoto, K., Uema, M., Sagara, H., Tanaka, M., Sata, T., Hashimoto, Y., and Kawaguchi, Y. (2008). Simultaneous tracking of capsid, tegument, and envelope protein localization in living cells infected with triply fluorescent herpes simplex virus 1. J Virol *82*, 5198-5211.

Sunayama, J., Ando, Y., Itoh, N., Tomiyama, A., Sakurada, K., Sugiyama, A., Kang, D., Tashiro, F., Gotoh, Y., Kuchino, Y., and Kitanaka, C. (2004). Physical and functional interaction between BH3-only protein Hrk and mitochondrial pore-forming protein p32. Cell Death Differ *11*, 771-781.

Suppiah, S., Mousa, H. A., Tzeng, W. P., Matthews, J. D., and Frey, T. K. (2012). Binding of cellular p32 protein to the rubella virus P150 replicase protein via PxxPxR motifs. J Gen Virol *93*, 807-816.

Tanaka, M., Kagawa, H., Yamanashi, Y., Sata, T., and Kawaguchi, Y. (2003). Construction of an excisable bacterial artificial chromosome containing a full-length infectious clone of herpes simplex virus type 1: viruses reconstituted from the clone exhibit wild-type properties in vitro and in vivo. J Virol *77*, 1382-1391.

Toropova, K., Huffman, J. B., Homa, F. L., and Conway, J. F. (2011). The herpes simplex virus 1 UL17 protein is the second constituent of the capsid vertex-specific component required for DNA packaging and retention. J Virol *85*, 7513-7522.

van Leeuwen, H. C., and O'Hare, P. (2001). Retargeting of the mitochondrial protein p32/gC1Qr to a cytoplasmic compartment and the cell surface. J Cell Sci *114*, 2115-2123.

Van Scoy, S., Watakabe, I., Krainer, A. R., and Hearing, J. (2000). Human p32: a coactivator for Epstein-Barr virus nuclear antigen-1-mediated transcriptional

activation and possible role in viral latent cycle DNA replication. Virology *275*, 145-157.

Wisner, T. W., Wright, C. C., Kato, A., Kawaguchi, Y., Mou, F., Baines, J. D., Roller, R. J., and Johnson, D. C. (2009). Herpesvirus gB-induced fusion between the virion envelope and outer nuclear membrane during virus egress is regulated by the viral US3 kinase. J Virol *83*, 3115-3126.

Yang, K., and Baines, J. D. (2011). Selection of HSV capsids for envelopment involves interaction between capsid surface components pUL31, pUL17, and pUL25. Proc Natl Acad Sci U S A *108*, 14276-14281.

Yu, L., Loewenstein, P. M., Zhang, Z., and Green, M. (1995). In vitro interaction of the human immunodeficiency virus type 1 Tat transactivator and the general transcription factor TFIIB with the cellular protein TAP. J Virol *69*, 3017-3023.

Zhang, Y., Sirko, D. A., and McKnight, J. L. (1991). Role of herpes simplex virus type 1 UL46 and UL47 in alpha TIF-mediated transcriptional induction: characterization of three viral deletion mutants. J Virol *65*, 829-841.

Acknowledgements

First and foremost, I would like to express my deepest heartfelt gratitude to my supervisor Professor Yasushi Kawaguchi for his continual guidance, words of wisdom, and friendship. He has been by my side in every difficult moment and provided me with much more support and understanding than one could possibly expect from a PhD supervisor. Without his support, the completion of this doctorate would have been impossible. I would also like to thank Dr. Akihisa Kato and Dr. Jun Arii for their excellent supervision and encouragement. Members of The Institute of Medical Science, especially the staffs and students of the Kawaguchi Laboratory have been invaluable in their support throughout my doctorate. It has been my honor and privilege to have learnt from and worked alongside you all.

My wonderful parents instilled in me that I am capable of achieving anything I set my mind to. Their exemplary hard work and innumerable sacrifices have allowed me so many opportunities in life, for this I am eternally grateful. To my beloved wife, she has been there for me all the time, with a dedication that is beyond any words.

Finally, I would like to acknowledge the financial support of Japanese Government MEXT (Ministry of Education, Culture, Sports, Science, and Technology)

Scholarship (2010/10-2015/3).

Figures

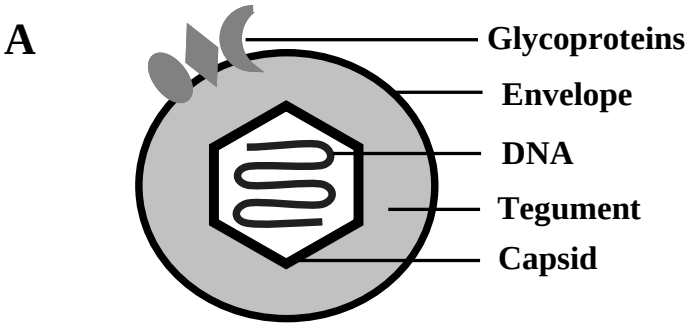

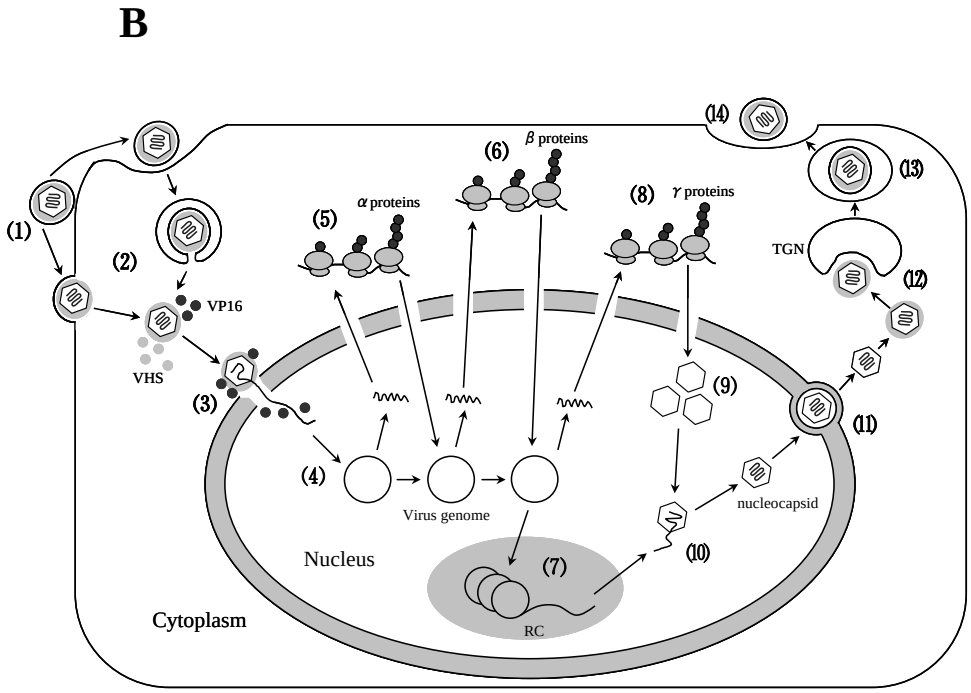

Fig. 1. Diagrams of the replication cycle of herpesvirus. (A) Model of herpesvirus virion. The Glycoprotein, envelope, tegument, capsid, DNA are indicated. (B) The life cycle of herpesvirus. (1): The virus binds to the cell plasma membrane and the virion envelope fuses with the plasma membrane or the virus enters by endocytosis (2), releasing the capsid and tegument proteins into the cytoplasm. VP16 localizes into the nucleus and VHS protein causes degradation of host messenger RNAs in the cytoplasm. (3): The capsid is transported to the nuclear pore, where the viral DNA is released into the nucleus. (4): The viral DNA circularizes. (5): Transcription and expression of α gene. α gene transcription is stimulated by the VP16 tegument protein. (6): Transcription and expression of β gene. α proteins transactivate β gene transcription.

(7): Replication of the viral DNA molecule. The β proteins are involved in replicating the viral DNA molecule. (8): Viral DNA synthesis stimulates γ gene expression. (9): The γ proteins are involved in assembling the capsid in the nucleus. (10): DNA is encapsidated in the capsid. (11): The filled capsids undergo primary envelopment at the inner nuclear membrane, become de-enveloped at the outer nuclear membrane and across the nuclear membrane. (12): In the cytosol, capsids are decorated and then bud into trans-Golgi network TGN. (13): Mature enveloped virion is formed (14): release ofvirions.

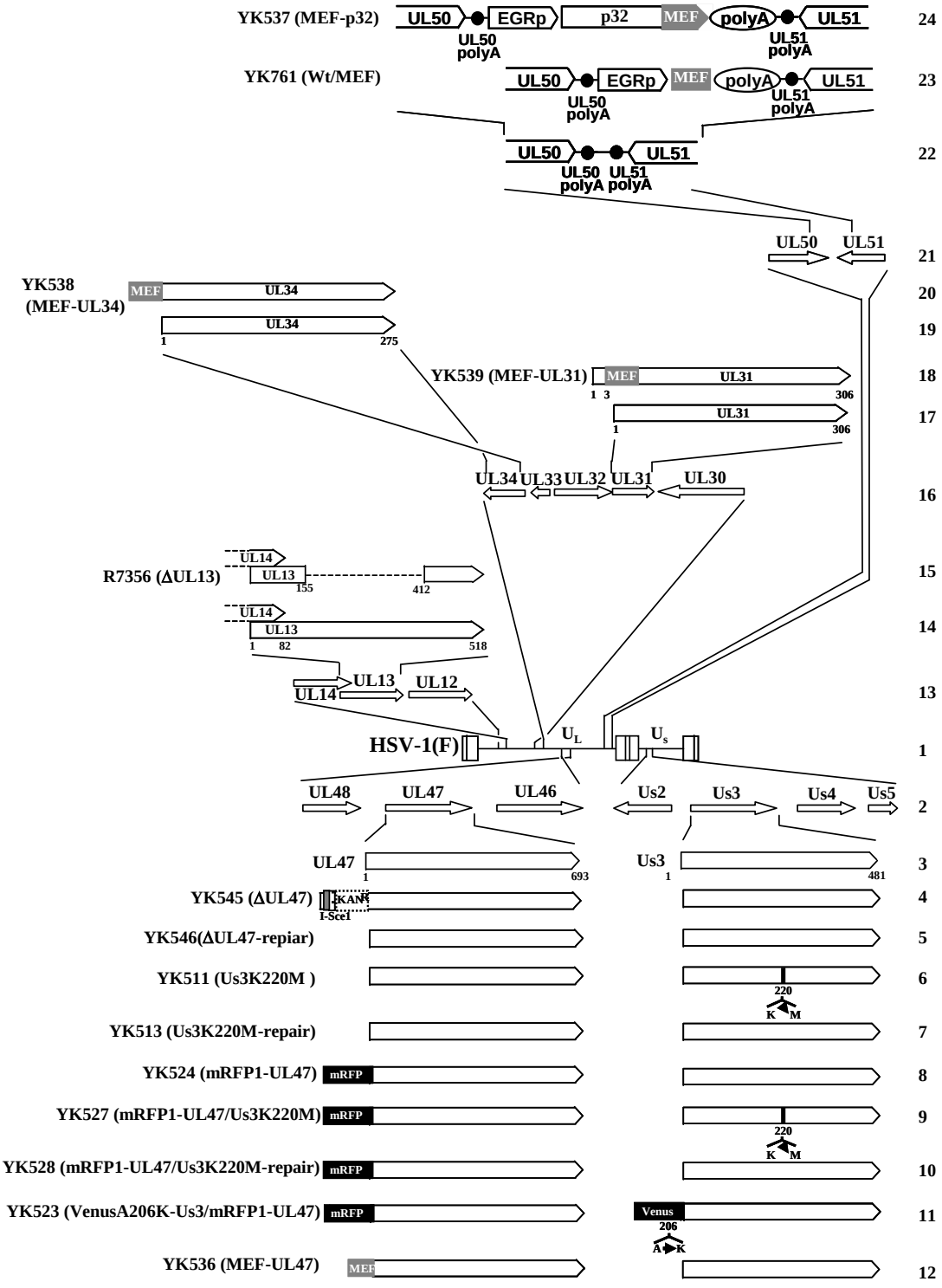

Fig.2. Schematic diagrams of the genome structures of wild-type HSV-1(F) and the relevant domains of the recombinant viruses used in this study. Line 1, Wild-type HSV-1(F) genome. Line 2, domains with the UL46 to UL48 and Us2 to Us5 genes. Line 3, domains of the UL47 and Us3 genes. Lines 4 to 12, recombinant viruses with

mutations in the UL47 and/or Us3 genes. Line 13, domain with the UL12 to UL14 genes. Line 14, domains with the UL13 gene and a part of the UL14 gene. Line 15, recombinant virus with a null-mutation in the UL13 gene. Line 16, domains with the UL30 to UL34 genes. Line 17, domain with the UL31 gene. Line 18, recombinant virus encoding MEF-tagged UL31. Line 19, domain with the UL34 gene. Line 20, recombinant virus encoding MEF-tagged UL34. Line 21, domain with the UL50 and UL51 genes. Line 22, intergenic region between UL50 and UL51 genes. Lines 23 and 24, recombinant viruses in which the expression cassette with the MEF-tag or MEF-tagged p32 was inserted into the intergenic region between UL50 and UL51, respectively.

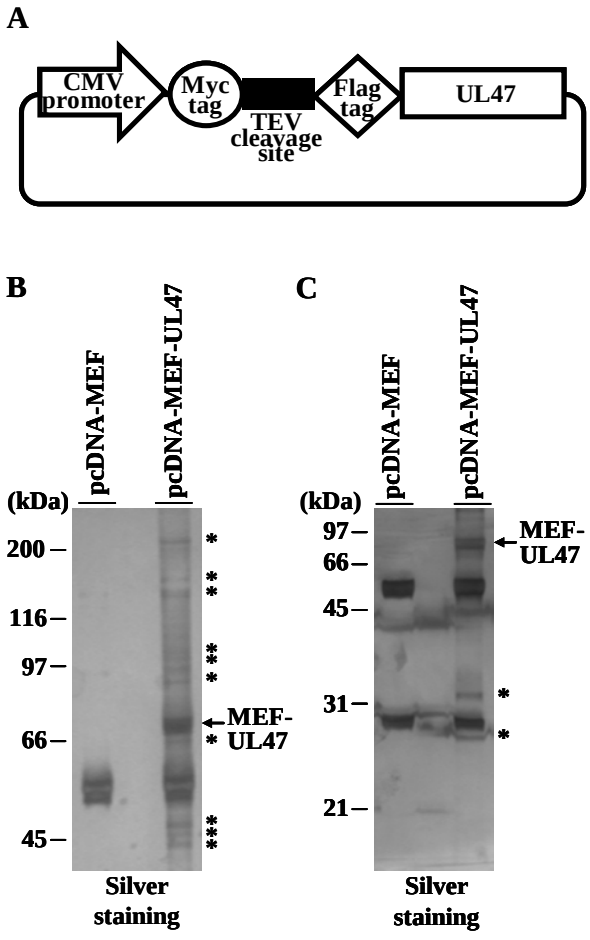

Fig.3. Identification of cellular proteins interacting with HSV-1 UL47. (A) Schematic of expression plasmid pcDNA-MEF-UL47 encoding UL47 fused to an MEF tag. (B) 293T cells were transfected with the empty vector pcDNA-MEF or plasmid pcDNA-MEF-UL47, harvested, and immunoprecipitated with anti-Myc antibody and

anti-Flag antibody. Immunoprecipitates were separated in 7.5% (B) or 12% (C) denaturing gels and silver stained. Bands marked with asterisks were excised, digested and analyzed by mass spectrometry. The arrow marks MEF-UL47. Molecular mass markers are indicated on the left.

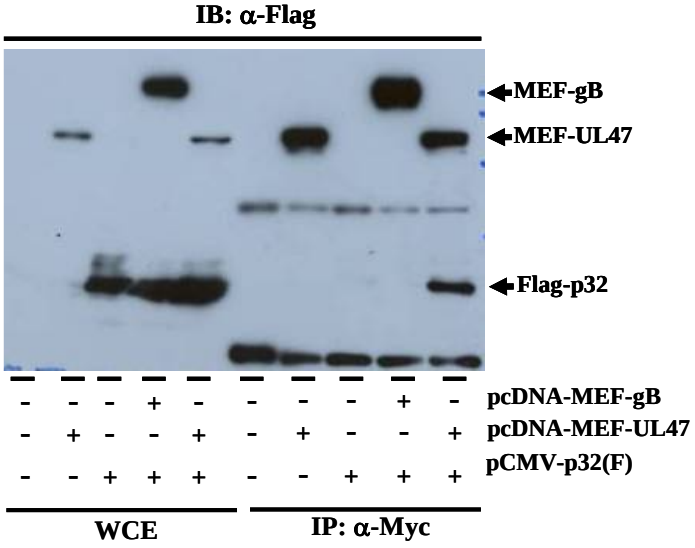

Fig.4. Interaction of UL47 with p32 in cell cultures. 293T cells were mock-transfected or transfected with pcDNA-MEF-UL47 alone, pCMV-p32(F) encoding Flag tagged p32 alone, or pCMV-p32(F) in combination with either pcDNA-MEF-UL47 or pcDNA-MEF-gB. At 2 d post-transfection, cells were harvested, immunoprecipitated (IP) with anti-Myc antibody (α-Myc), and analyzed by immunoblotting (IB) with anti-Flag antibody (α-Flag). WCE, whole-cell extract.

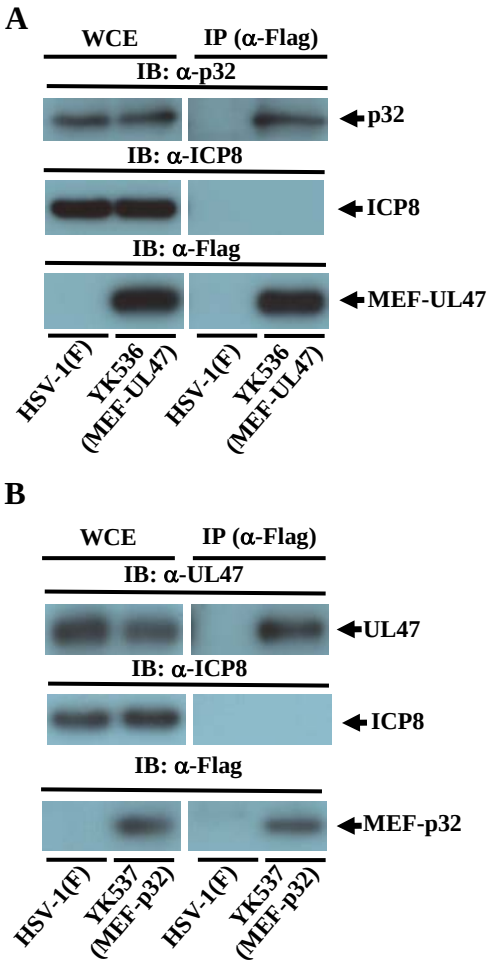

Fig. 5. Interaction of UL47 with p32 in HSV-1-infected cells. (A) Vero cells infected with wild-type HSV-1(F) or YK536 (MEF-UL47) at an MOI of 5 for 18 h were harvested, immunoprecipitated (IP) with anti-Flag antibody (α-Flag), and analyzed by immunoblotting (IB) with anti-p32 antibody (α-p32), anti-ICP8 antibody (α-ICP8), or anti-Flag antibody. WCE, whole-cell extract. (B) Vero cells infected with wild-type HSV-1(F) or YK537 (MEF-p32) at an MOI of 5 for 18 h were harvested, immunoprecipitated (IP) with anti-Flag antibody (α-Flag), and analyzed by immunoblotting (IB) with anti-UL47 antibody (α-UL47), anti-ICP8 antibody (α-ICP8), or anti-Flag antibody. WCE, whole cell extract.

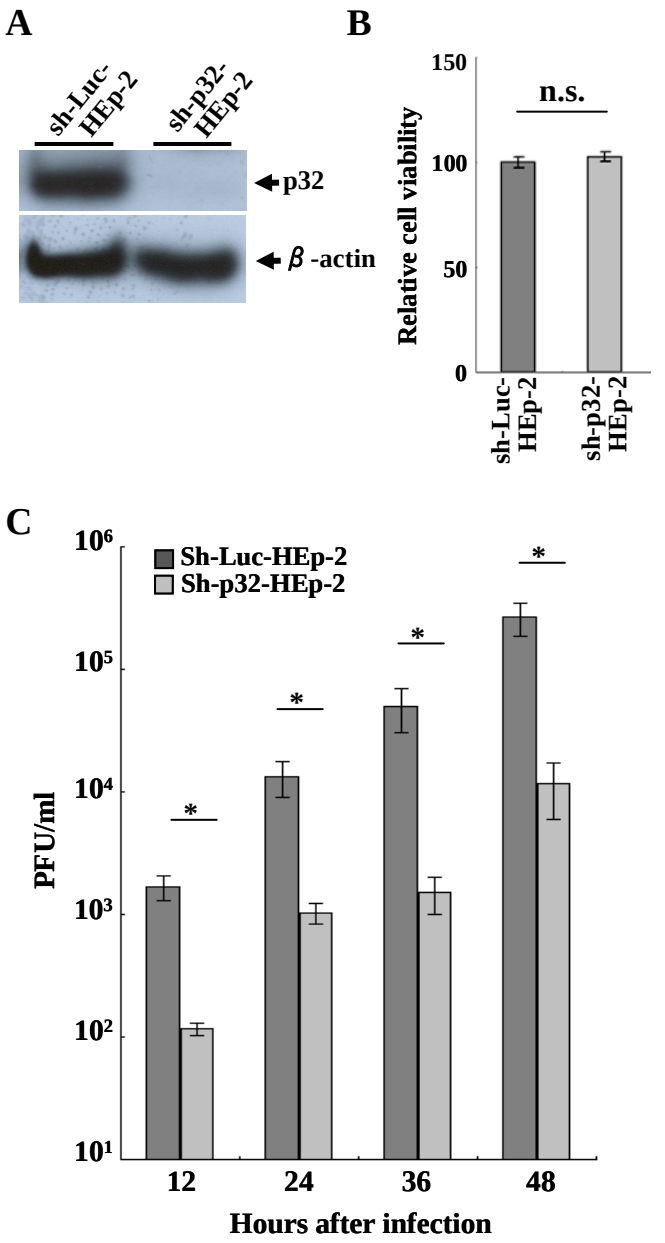

Fig. 6. Effect of p32 on HSV-1 replication in cell cultures. (A) Expression of p32 in sh-Luc-HEp-2 and sh-p32-HEp-2 cells analyzed by immunoblotting with anti-p32 (top) and anti-βactin (bottom) antibodies. (B) Cell viability of sh-Luc-HEp-2 and sh-p32-HEp-2 cells assayed 24 h after $2x10^4$ cells were seeded on 96-well plates. Each value is the mean ± standard error of the results of triplicate experiments and is expressed relative to the mean for sh-Luc-HEp-2 cells, which was normalized to 100%. n.s.; not statistically significant. Data are representative of three independent experiments. (C) sh-Luc-HEp-2 and sh-p32-HEp-2 cells were infected with wild-type HSV-1(F) at an MOI of 0.01. At the indicated times post-infection, total

virus from cell culture supernatants and infected cells was harvested and assayed on Vero cells. Each value is the mean ± the standard error of the results of triplicate experiments. Asterisks indicate statistically significant differences (*, $P < 0.05$). Data are representative of three independent experiments.

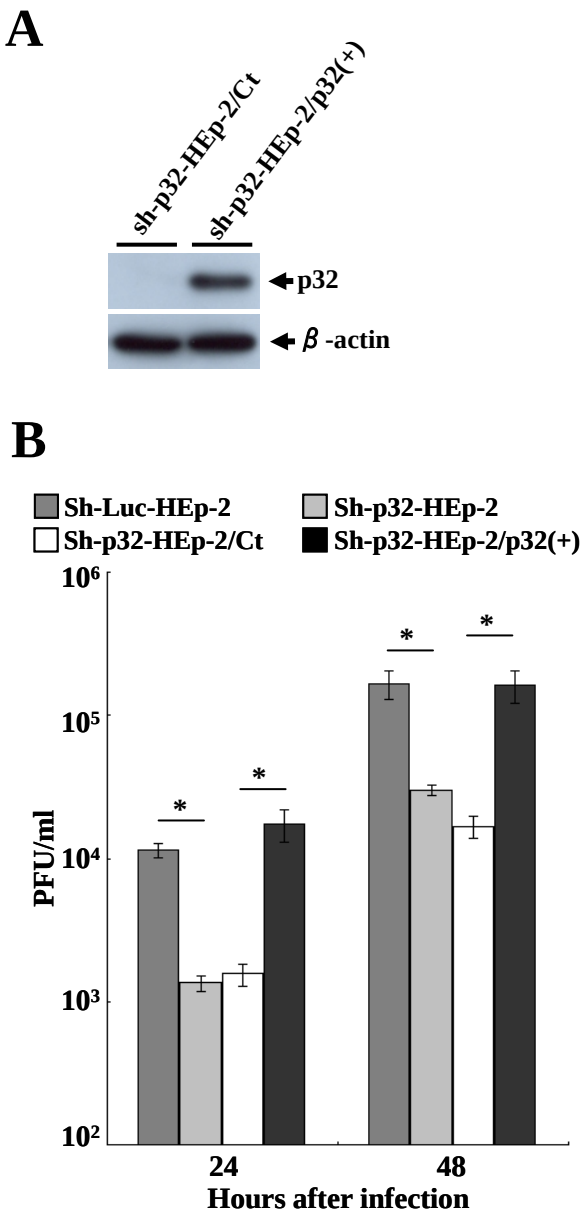

Fig. 7. Effect of p32 overexpression on HSV-1 replication in sh-p32-HEp-2 cells. (A) Expression of p32 in sh-p32-HEp-2/Ct and sh-p32-HEp-2/(p32+) cells analyzed by immunoblotting with anti-p32 (top) and anti-βactin (bottom) antibodies. (B) sh-Luc-HEp-2, sh-p32-HEp-2, sh-p32-HEp-2/Ct and sh-p32-HEp-2/p32(+) cells were

infected with wild-type HSV-1(F) at an MOI of 0.01. At 24 and 48 h post-infection, total virus from cell culture supernatants and infected cells was harvested and assayed on Vero cells. Each value is the mean ± standard error of the results of triplicate experiments. Asterisks indicate statistically significant differences (*, $P < 0.05$). Data are representative of three independent experiments.

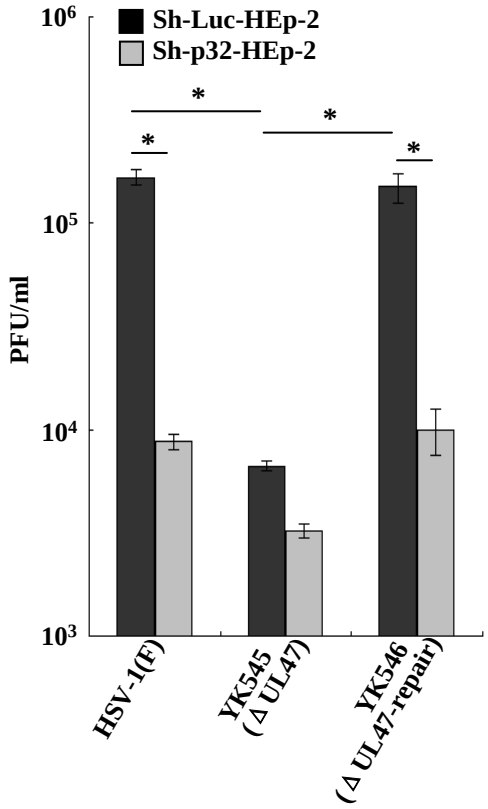

Fig. 8. Effect of p32 in combination with UL47 on HSV-1 replication in cell cultures. sh-Luc-HEp-2 and sh-p32-HEp-2 cells were infected with wild-type HSV-1(F), YK545 (ΔUL47) or YK546 (ΔUL47-repair) at an MOI of 0.01. At 24 h post-infection, total virus from cell culture supernatants and infected cells was harvested and assayed on Vero cells. Each value is the mean ± standard error of the results of triplicate experiments. Asterisks indicate statistically significant differences (*, $P < 0.05$). Data are representative of three independent experiments.

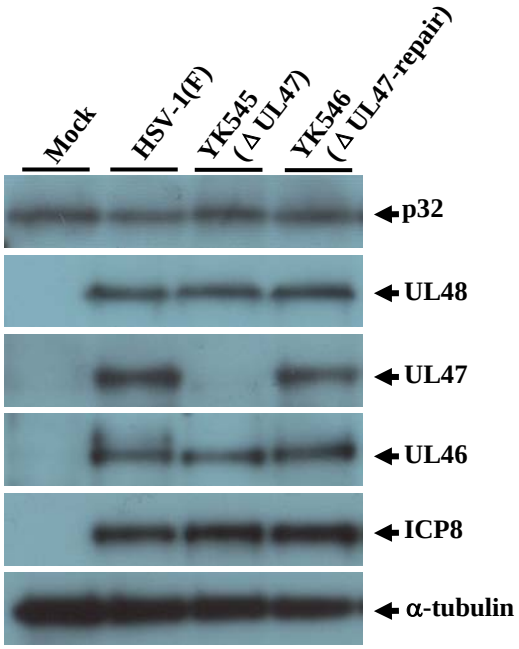

Fig. 9. Effect of the null-mutation in UL47 on expression of neighboring genes UL48 and UL46. Vero cells were mock-infected or infected with wild-type HSV-1(F), YK545 (ΔUL47), or YK456 (ΔUL47-repair) at an MOI of 5, harvested at 18 h post-infection, lysed, and analyzed by immunoblotting with antibodies to the indicated proteins.

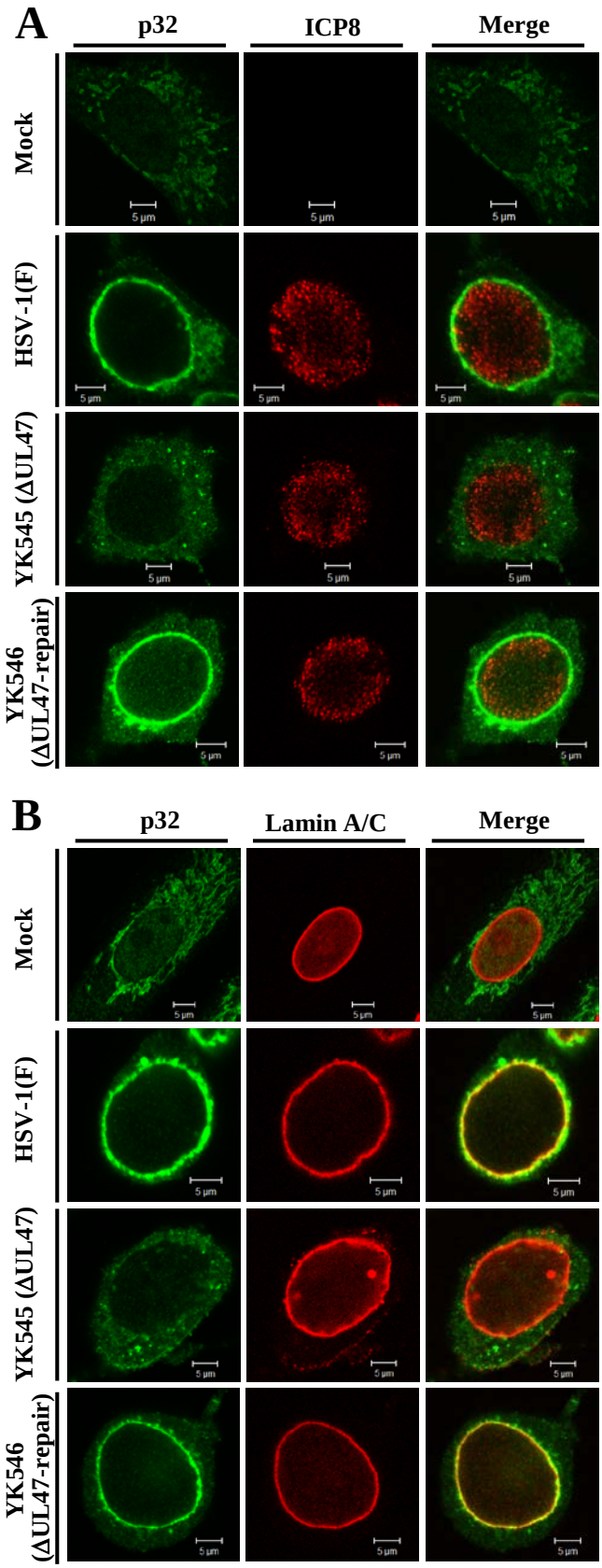
A
p32
ICP8
Merge
Mock
HSV-1(F)
YK545 (ΔUL47)
YK546 (ΔUL47-repair)
5 μm
B
p32
Lamin A/C
Merge
Mock
HSV-1(F)
YK545 (ΔUL47)
YK546 (ΔUL47-repair)
5 μm

Fig. 10. Localization of p32 in HSV-1-infected cells and effect of UL47 on p32 localization. (A) Vero cells mock-infected or infected with wild-type HSV-1 (F), YK545 (ΔUL47) or YK546 (ΔUL47-repair) at an MOI of 3 were fixed at 18 h post-infection, permeabilized, stained with anti-p32 antibody or anti-ICP8 antibody, and examined by confocal microscopy. (B) Experiments were done by the same procedure as in (A), except anti-lamin A/C antibody was used instead of anti-ICP8 antibody.

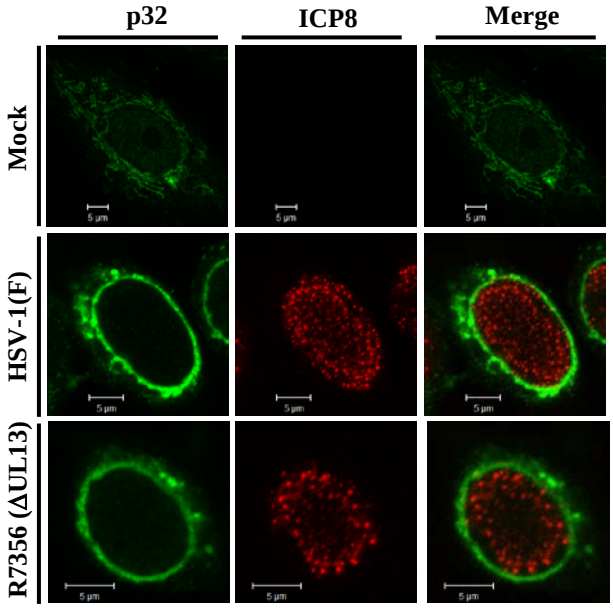

Fig. 11. Effect of UL13 on p32 localization in HSV-1-infected cells. Vero cells mock-infected or infected with wild-type HSV-1 (F) or R7356 (ΔUL13) at an MOI of 3 were fixed at 18 h post-infection, permeabilized, stained with anti-p32 antibody or anti-ICP8 antibody, and examined by confocal microscopy.

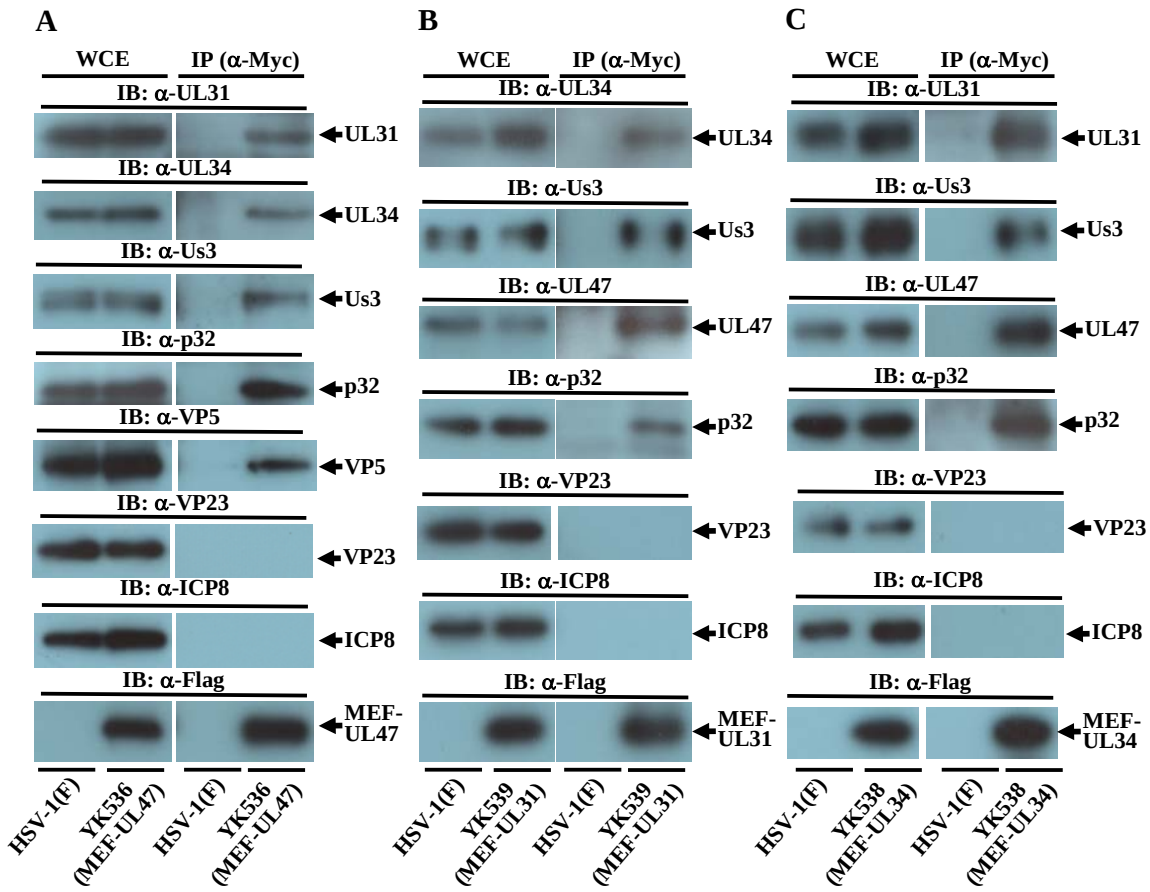

Fig. 12. Interactions among UL47, p32, UL31, UL34 and Us3 in HSV-1-infected cells. Vero cells infected with wild-type HSV-1(F) (A to C), YK536 (MEF-UL47) (A), YK539 (MEF-UL31) (B) or YK538 (MEF-UL34) (C) at an MOI of 5 for 18 h were harvested, immunoprecipitated (IP) with anti-Myc antibody (α-Myc), and analyzed by immunoblotting (IB) with the indicated antibodies. WCE, whole-cell extract.

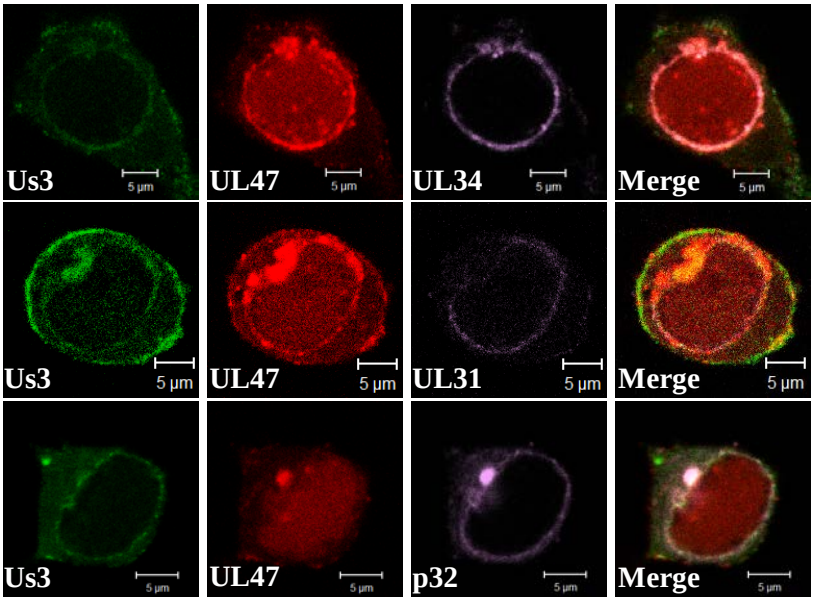

Fig. 13. Localization of Us3, UL47, UL34, UL31 and p32 in HSV-1-infected cells. Vero cells were infected with YK523 (mRFP-UL47/Venus-Us3) at an MOI of 3, fixed at 18 h post-infection, permeabilized, stained with anti-UL34 (top panels), anti-UL31 (middle panels) or anti-p32 (bottom panels) antibody, and examined by confocal microscopy.

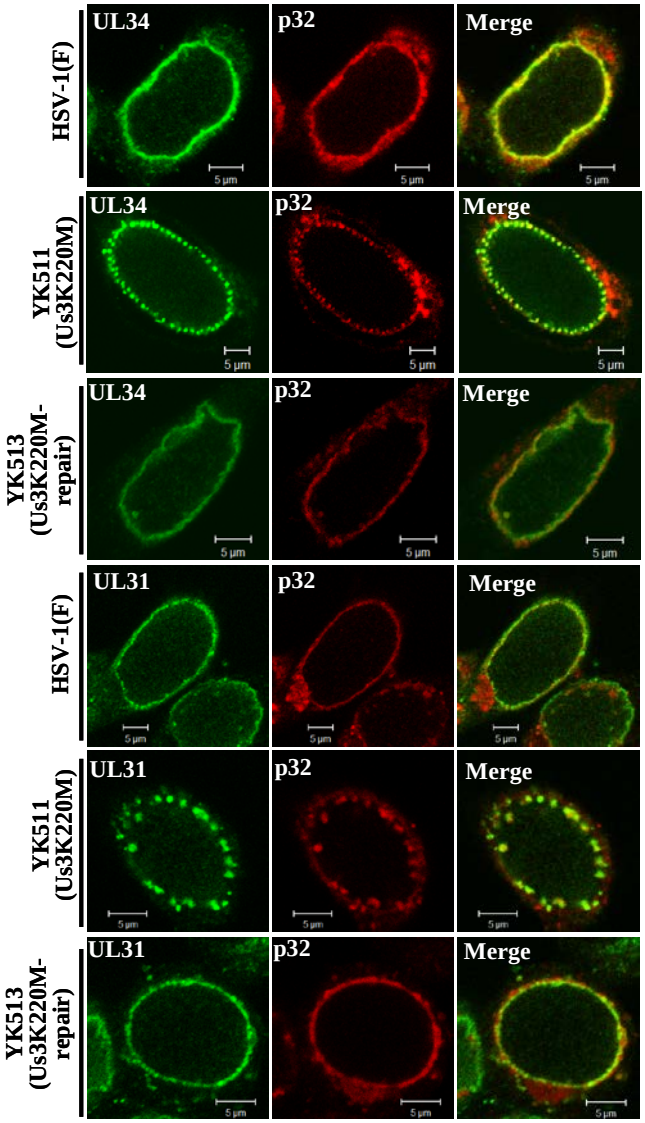

Fig. 14. Effect of Us3 kinase activity on localization of p32, UL34 and UL31 in HSV-1-infected cells. Vero cells were infected with wild-type HSV-1 (F), YK511 (Us3K220M) or YK513 (Us3K220M-repair) at an MOI of 3, fixed at 18 h post-infection, permeabilized, stained with anti-p32 antibody in combination with anti-UL34 or anti-UL31 antibody, and examined by confocal microscopy.

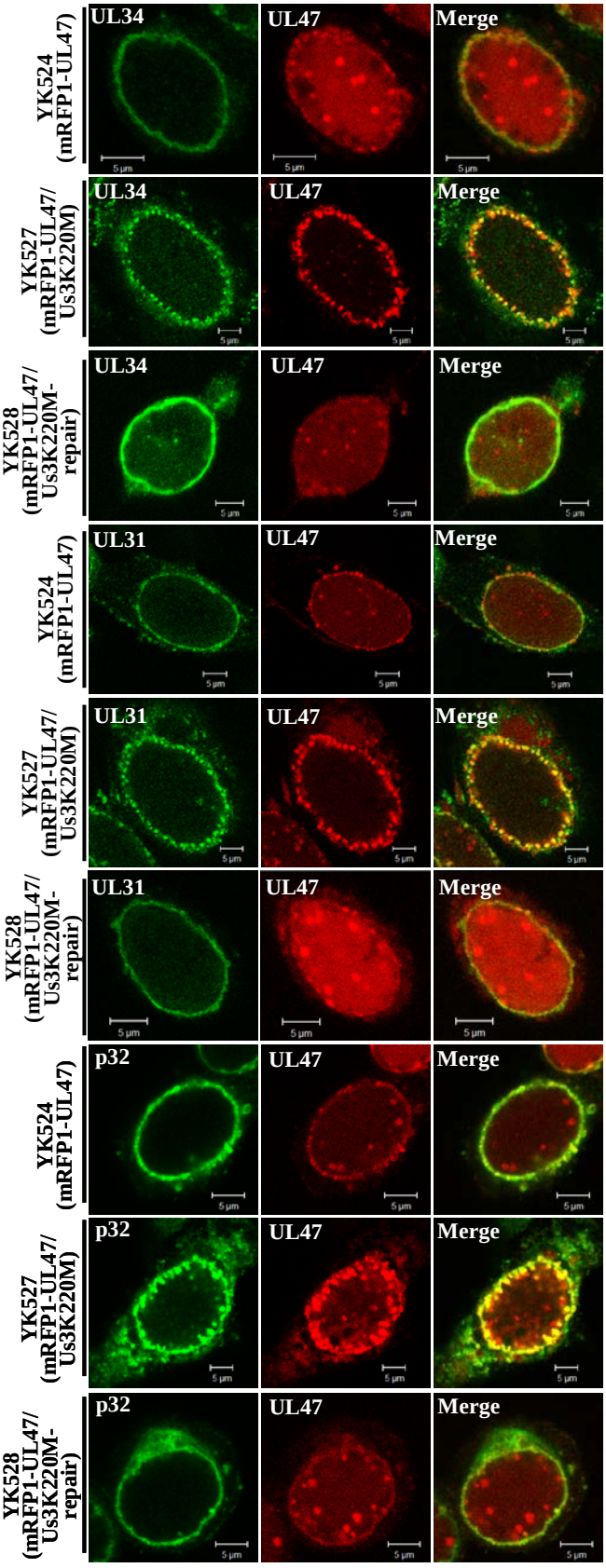

Fig. 15. Effect of Us3 kinase activity on localization of mRFP1-UL47, p32, UL34

and UL31 in HSV-1-infected cells. Vero cells were infected with YK524 (mRFP1-UL47), YK527 (mRFP1-UL47/Us3K220M) or YK528 (mRFP1-UL47/Us3K220M-repair) at an MOI of 3, fixed at 18 h post-infection, permeabilized, stained with anti-UL34, anti-UL31 or anti-p32 antibody, and examined by confocal microscopy.

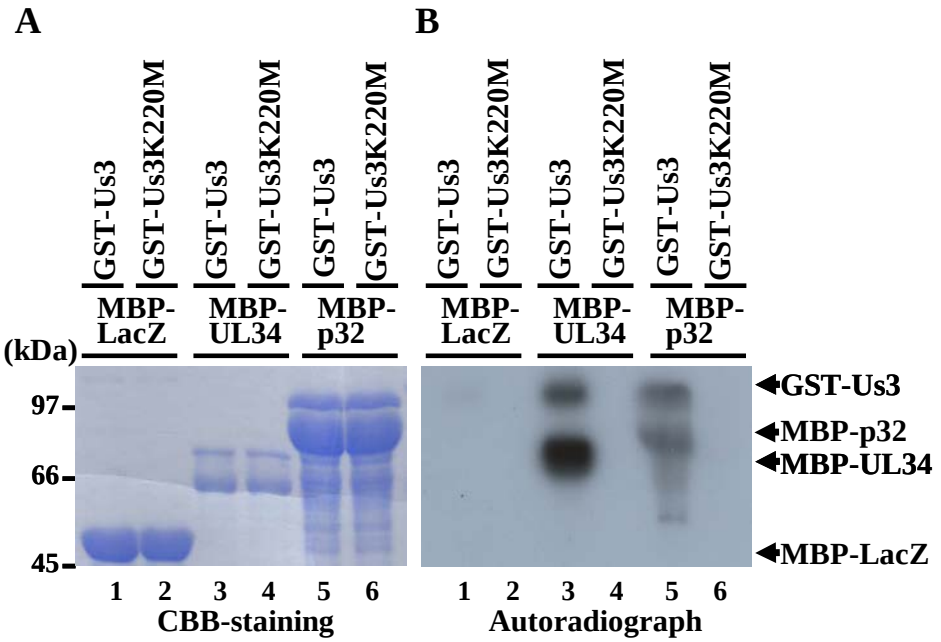

Fig. 16. Us3 phosphorylation of p32 in vitro. (A) Purified MBP-lacZ (lanes 1 and 2), MBP-UL34 (lanes 3 and 4) and MBP-p32 (lanes 5 and 6) were incubated in kinase buffer containing [γ-^{32}P] ATP and either purified GST-Us3 (lanes 1, 3 and 5) or GST-Us3K220M (lanes 2, 4 and 6), separated on a denaturing gel, and stained with CBB. (B) Autoradiograph of the gel in (A). Molecular mass markers are on the left.

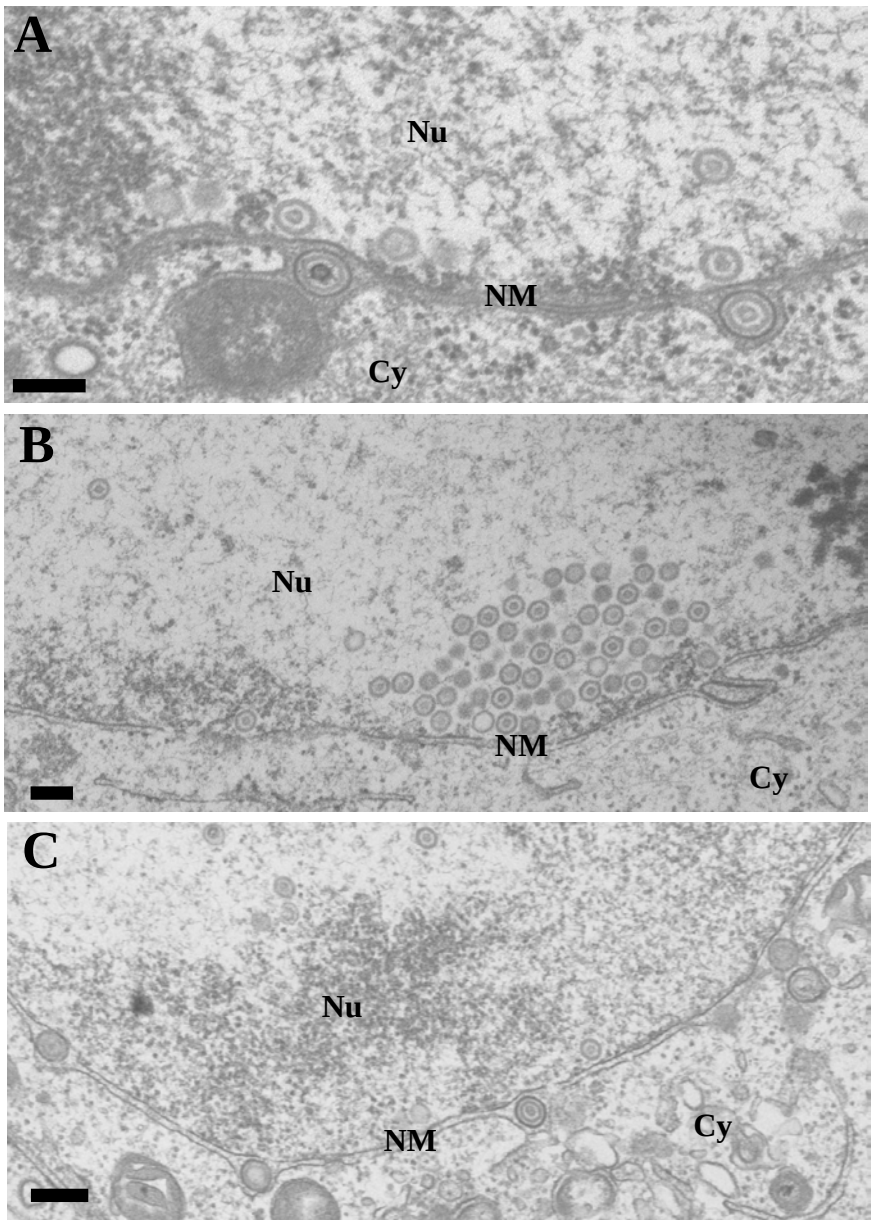

Fig. 17. Ultrastructural analysis of the effect of UL47 on HSV-1 nuclear egress. Vero cells infected with wild-type HSV-1(F) (A), YK545 (ΔUL47) (B) or YK546 (ΔUL47-repair) (C) at an MOI of 5 were fixed at 18 h post-infection, embedded, sectioned, stained, and examined by transmission electron microscopy. Nu, nucleus; Cy, cytoplasm; NM, nuclear membrane. Bars, 200 nm.

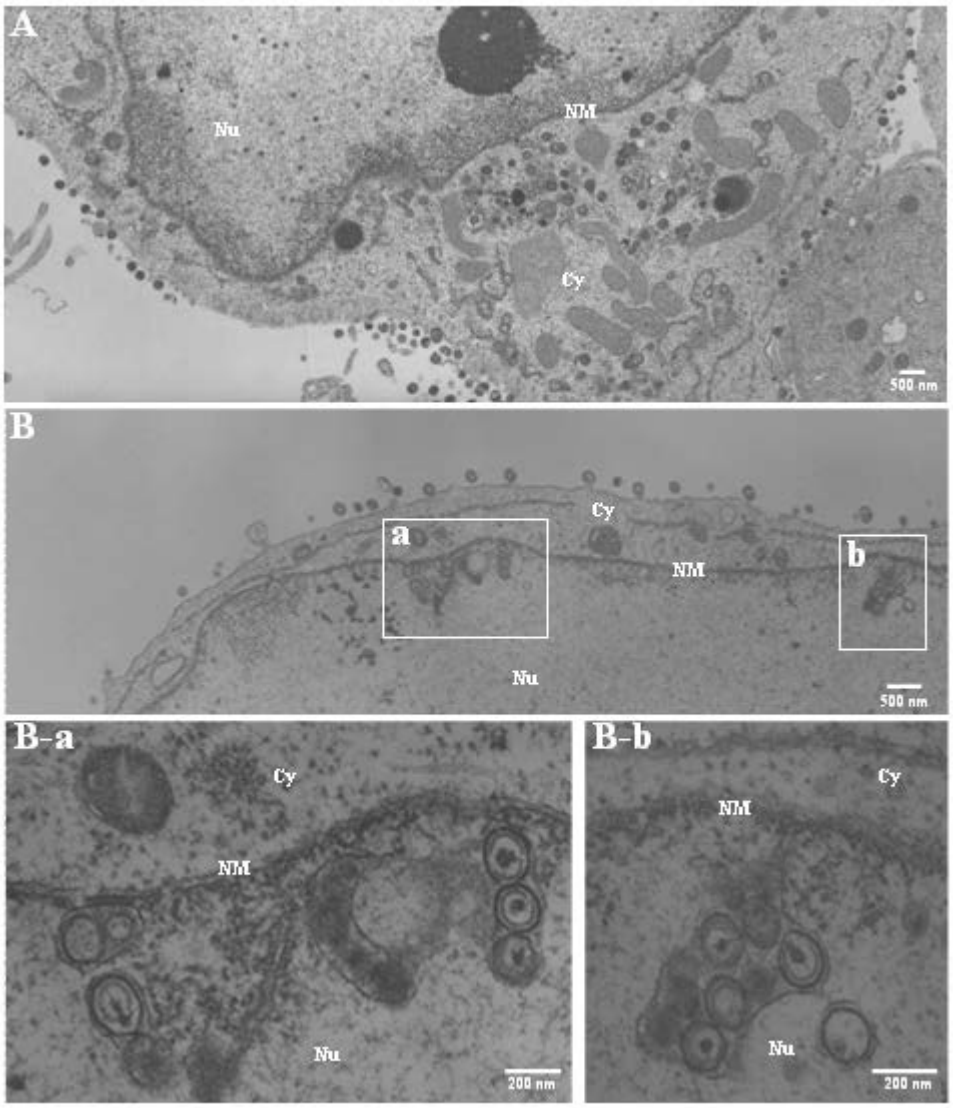

Fig. 18. Ultrastructural analysis of the effect of p32 on HSV-1 nuclear egress. sh-Luc-HEp-2 (A) and sh-p32-HEp-2 cells (B) infected with wild-type HSV-1 (F) at an MOI of 5 were fixed at 24 h post-infection, embedded, sectioned, stained, and examined by transmission electron microscopy. (B-a and B-b) Higher magnifications of the corresponding boxed areas in (B) showing invagination structures containing primary enveloped virions. Nu, nucleus; Cy, cytoplasm; NM, nuclear membrane.

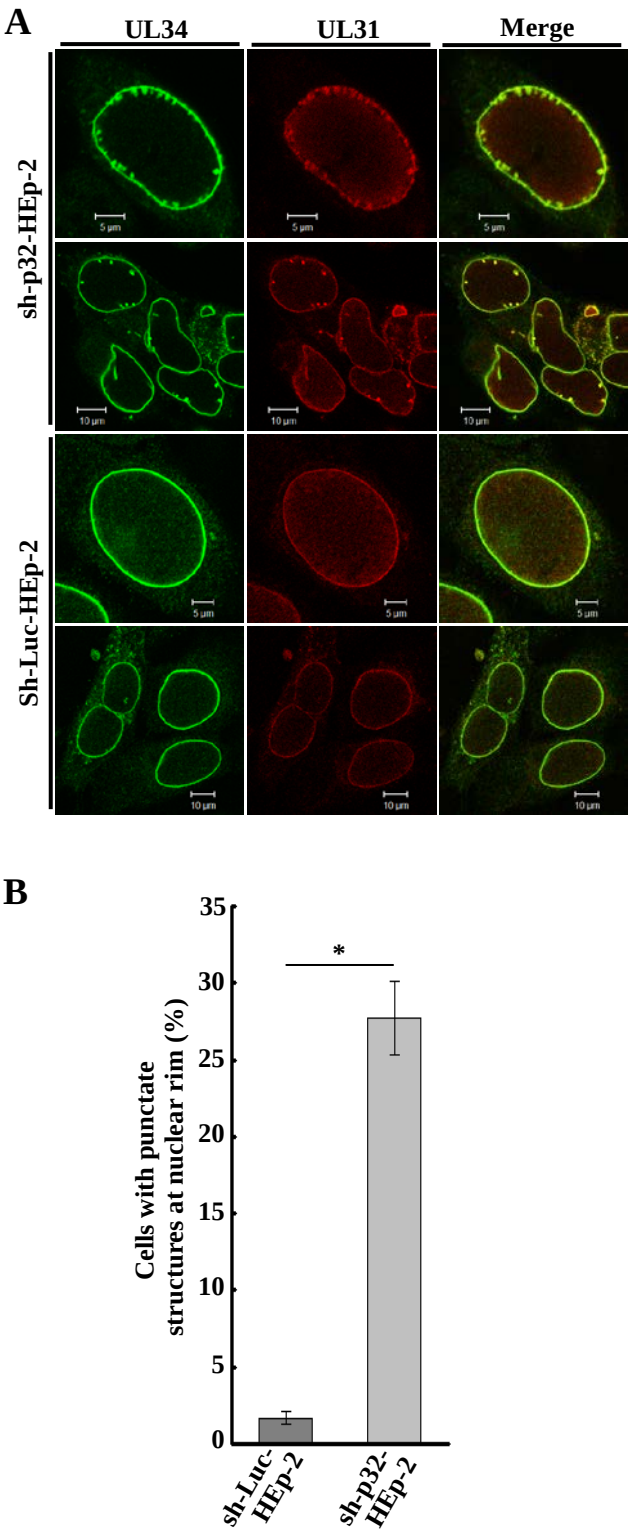

Fig. 19. Effect of p32 on localization of UL34 and UL31 in HSV-1-infected cells. (A) sh-p32-HEp-2 and sh-Luc-HEp-2 cells were infected with wild-type HSV-1 (F) at an MOI of 5, fixed at 24 h post-infection, permeabilized, stained with anti-UL34 and

anti-UL31 antibodies, and examined by confocal microscopy. (B) Quantification of infected cells showing aberrant punctate structures at the nuclear rim. Infected sh-p32-HEp-2 and sh-Luc-HEp-2 cells were examined by confocal microscopy as described for (A), and the percentage of cells with aberrant punctate structures at the nuclear rim was determined for 100-cell samples. Each value is the mean ± standard error of the results of triplicate experiments. Asterisks indicate statistically significant differences (*, $P < 0.05$). Data are representative of three independent experiments.

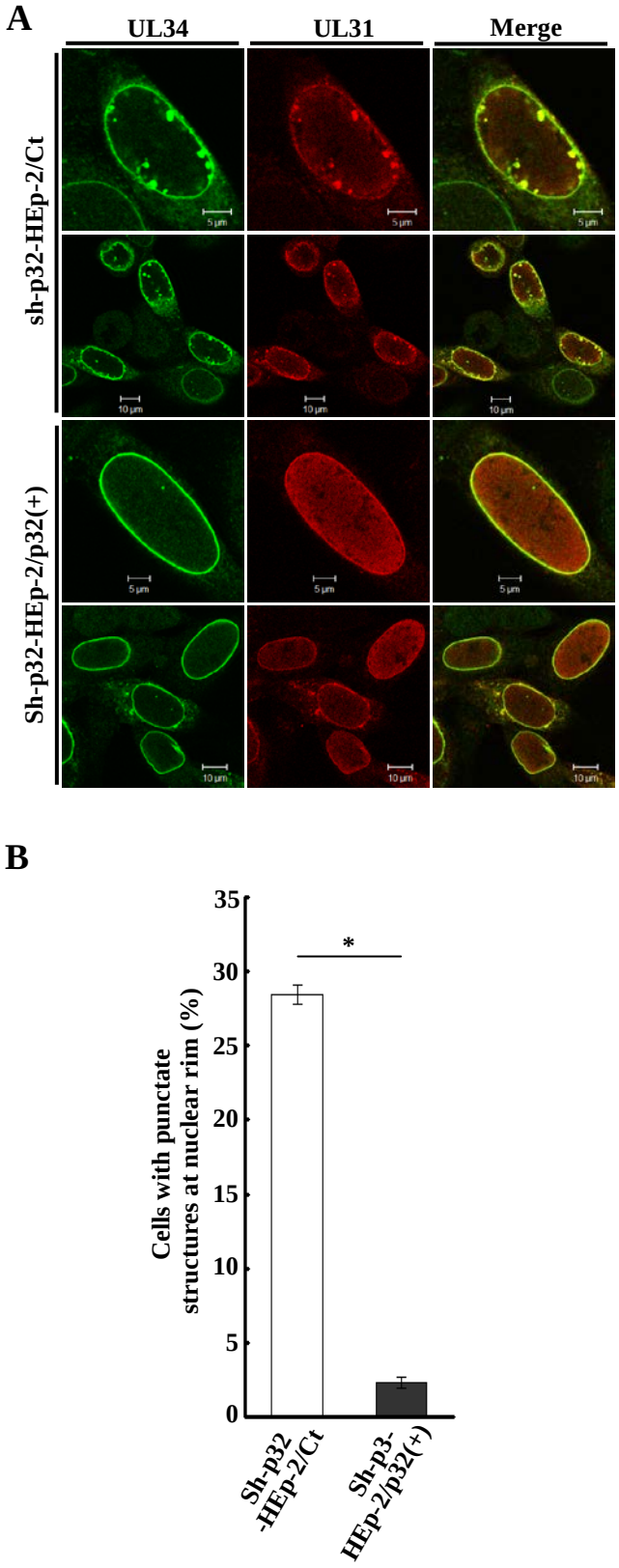

Fig. 20. Effect of p32 overexpression on localization of UL34 and UL31 in HSV-1-infected sh-p32-HEp-2 cells. (A) sh-p32-HEp-2/Ct and sh-p32-HEp-2/p32(+)

cells were infected with wild-type HSV-1 (F) at an MOI of 5, fixed at 24 h post-infection, permeabilized, stained with anti-UL34 and anti-UL31 antibodies, and examined by confocal microscopy. (B) Quantification of infected cells with aberrant punctate structures at the nuclear rim. Infected sh-p32-HEp-2/Ct and sh-p32-HEp-2/p32(+) cells were examined by confocal microscopy as described in (A), and the percentage of cells with aberrant punctate structures at the nuclear rim was determined for 100-cell samples. Each value is the mean ± standard error of the results of triplicate experiments. Asterisks indicate statistically significant differences (*, $P < 0.05$). Data are representative of three independent experiments.

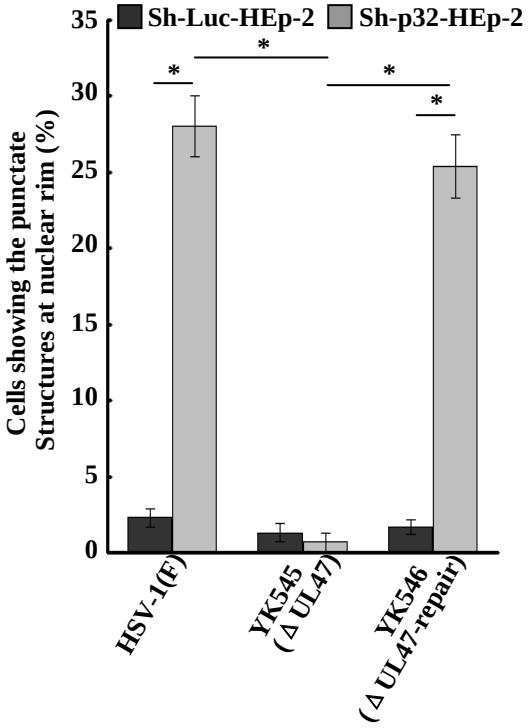

Fig. 21. Effect of p32 in combination with UL47 on localization of UL34 and UL31 in HSV-1-infected cells. sh-Luc-HEp-2 and sh-p32-HEp-2 cells were infected with wild-type HSV-1 (F), YK545 (ΔUL47) or YK546 (ΔUL47-repair) at an MOI of 5, fixed at 24 h post-infection, permeabilized, stained with anti-UL34 and anti-UL31 antibodies, and examined by confocal microscopy. The percentage of cells with aberrant punctate structures at the nuclear rim was determined for 100-cell samples. Each value is the mean ± standard error of the results of triplicate experiments. Asterisks indicate statistically significant differences (*, $P < 0.05$). Data are

representative of three independent experiments.

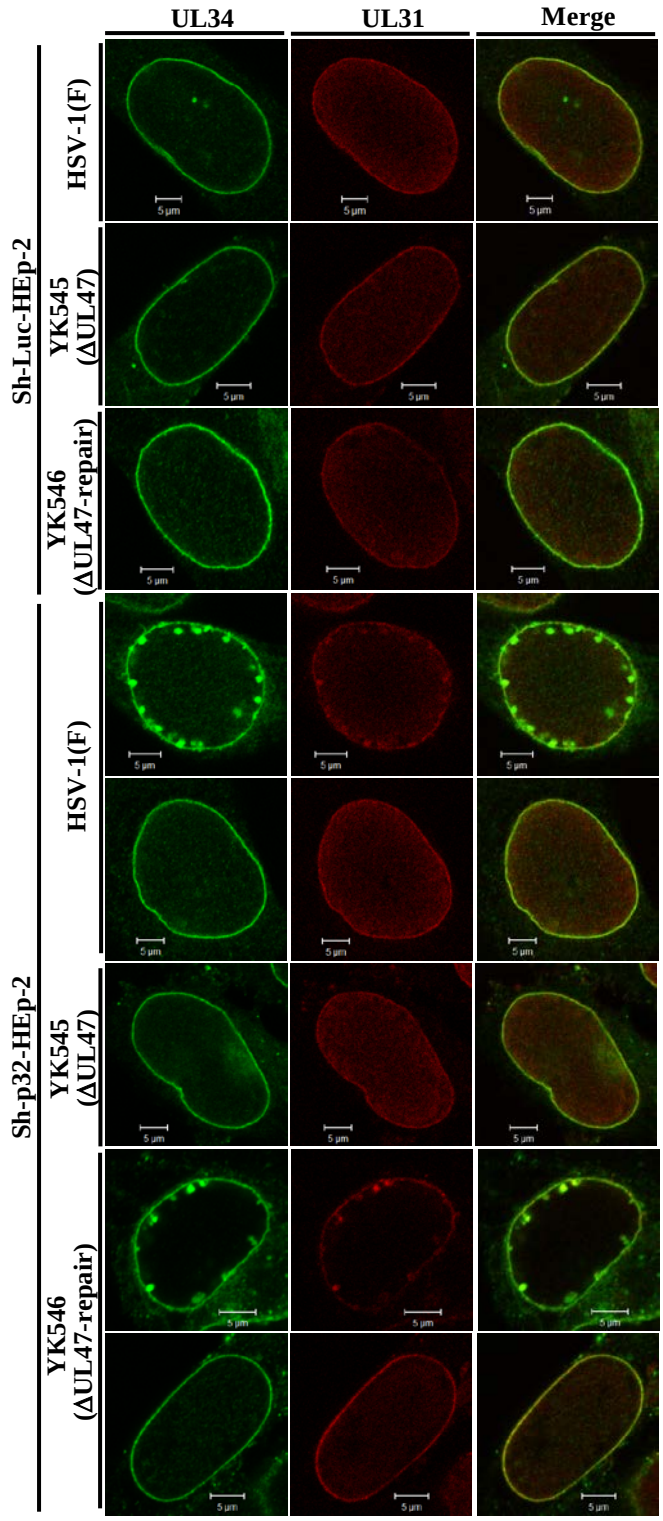

Fig. 22. Effect of p32 in combination with UL47 on localization of UL34 and UL31 in HSV-1-infected cells. sh-Luc-HEp-2 and sh-p32-HEp-2 cells were infected with

wild-type HSV-1 (F), YK545 (ΔUL47) or YK546 (ΔUL47-repair) at an MOI of 5, fixed at 24 h post-infection, permeabilized, stained with anti-UL34 and anti-UL31 antibodies, and examined by confocal microscopy.

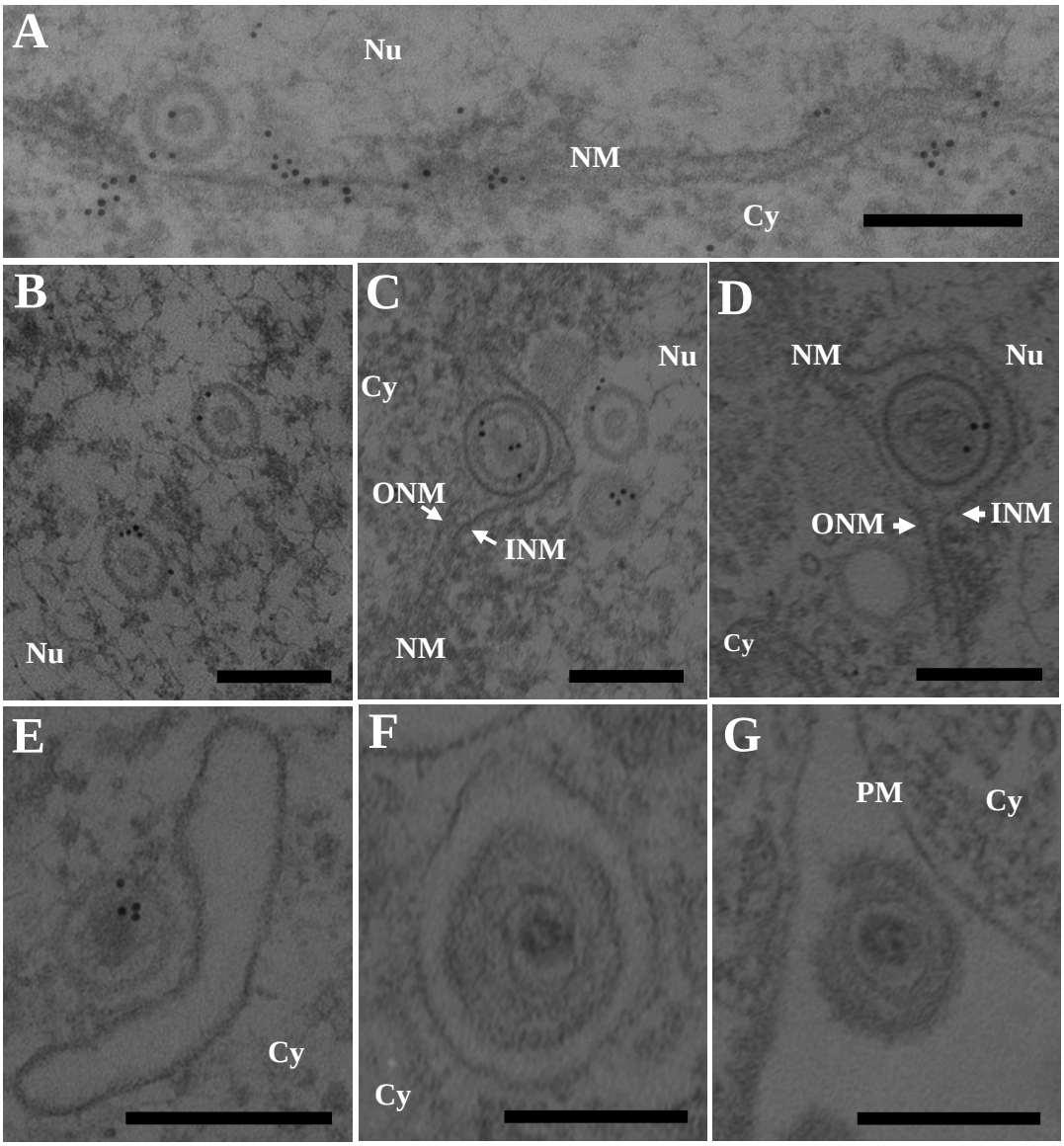

Fig. 23. Localization of p32 in HSV-1-infected cells by immunoelectron microscopy. Vero cells were infected with wild-type HSV-1(F) at an MOI of 5, fixed at 18 h post-infection, embedded, sectioned, stained with rabbit anti-p32 polyclonal antibody followed by goat anti-rabbit IgG conjugated onto 10-nm gold particles, and examined by transmission electron microscopy. Nu, nucleus; Cy, cytoplasm; NM, nuclear membrane; INM, inner nuclear membrane; ONM, outer nuclear membrane; PM, plasma membrane. p32 was detected along the nuclear membrane (A), on capsids in

the nucleus (A to C) and cytoplasm (E), and on primary enveloped virions in the perinuclear spaces (C and D), but was barely detectable on secondary enveloped virions in the cytoplasm (F) and in the extracellular space (G). Bars, 200 nm.

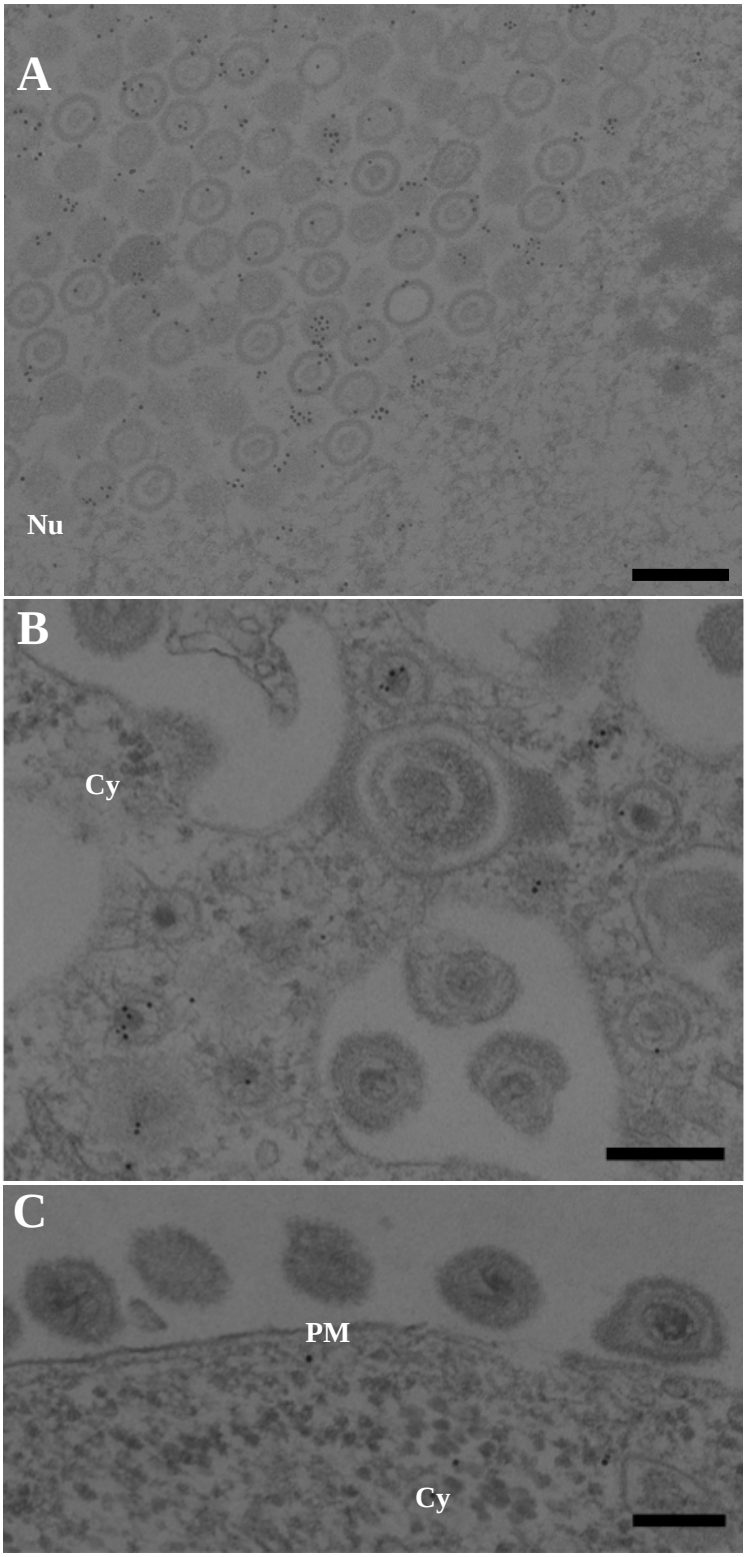

Fig. 24. Localization of p32 in HSV-1-infected cells by immunoelectron microscopy. Vero cells were infected with wild-type HSV-1(F) at an MOI of 5, fixed at 18 h post-infection, embedded, sectioned, stained with rabbit anti-p32 polyclonal antibody followed by goat anti-rabbit IgG conjugated onto 10-nm gold particles, and examined by transmission electron microscopy. Nu, nucleus; Cy, cytoplasm; NM, nuclear membrane; INM, inner nuclear membrane; ONM, outer nuclear membrane; PM, plasma membrane. p32 was detected on capsids in the nucleus (A) and cytoplasm (B), but was barely detected on secondary enveloped virions in the cytoplasm (B) and in the extracellular space (C). Bars, 200 nm.

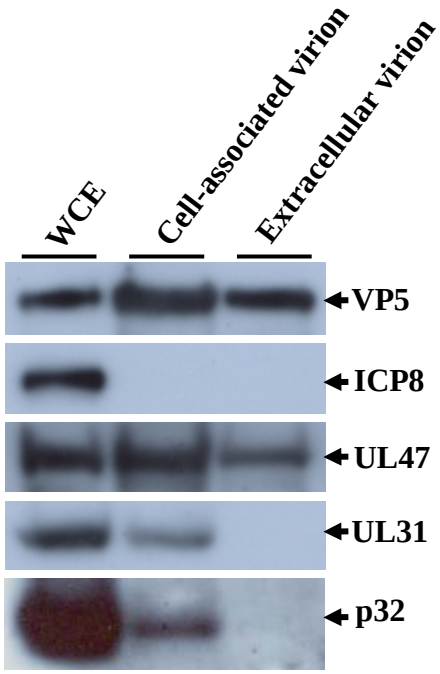

Fig. 25. Detection of p32 in cell-associated and extracellular virions. Cell-associated and extracellular virions were purified and analyzed by immunoblotting with antibodies to the indicated proteins. WCE, whole-cell extract.

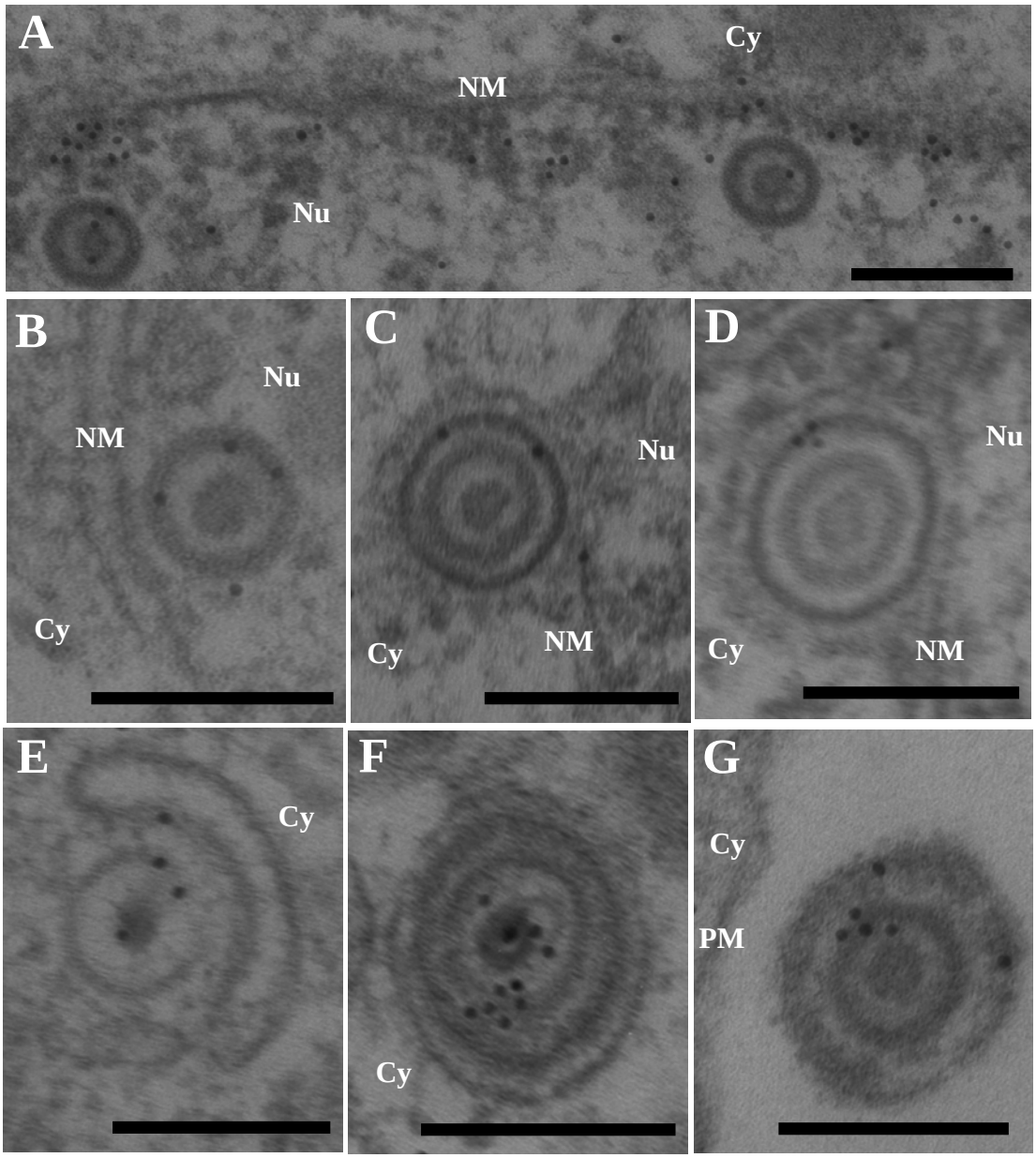

Fig. 26. Localization of UL47 in HSV-1-infected cells by immunoelectron microscopy. Vero cells were infected with YK536 (MEF-UL47) at an MOI of 5, fixed at 18 h post-infection, embedded, sectioned, stained with mouse anti-Myc monoclonal antibody followed by goat anti-mouse IgG conjugated onto 10-nm gold particles, and examined by transmission electron microscopy. Nu, nucleus; Cy, cytoplasm; NM, nuclear membrane; PM, plasma membrane. UL47 was detected in the nucleoplasm (A), along the nuclear membrane (A), on capsids in the nucleus (A and B) and cytoplasm (E), on primary enveloped virions in the perinuclear space (C and D), and on secondary enveloped virions in the cytoplasm (F) and extracellular

space (G). Bars, 200 nm.

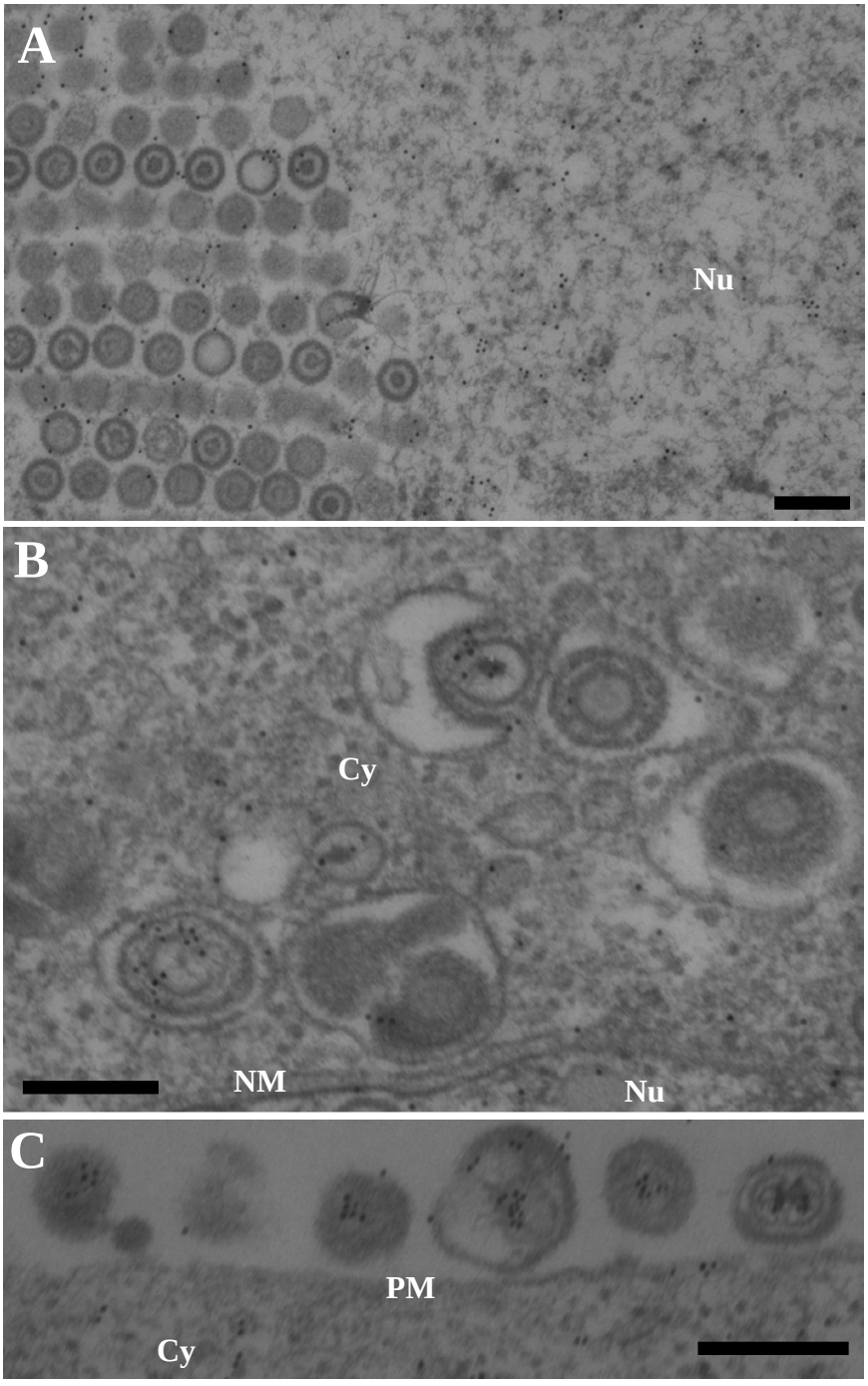

Fig. 27. Localization of UL47 in HSV-1-infected cells by immunoelectron microscopy. Vero cells were infected with YK536 (MEF-UL47) at an MOI of 5, fixed at 18 h post-infection, embedded, sectioned, stained with mouse anti-Myc monoclonal antibody followed by goat anti-mouse IgG conjugated onto 10-nm gold particles, and examined by transmission electron microscopy. Nu, nucleus; Cy, cytoplasm; NM,

nuclear membrane; PM, plasma membrane. UL47 was detected in the nucleoplasm (A), on capsids in the nucleus (A) and cytoplasm (B), and on secondary enveloped virions in the cytoplasm (B) and extracellular space (C). Bars, 200 nm.

Table 1. Host cellular proteins that co-immunoprecipitated with MEF-UL47

RefSeq accession number	Definition (gene symbol)	Score[a]	Peptide sequence	Predicted mass (Da)	SDS-PAGE mass (Da)
NP_004332.2	Carbamoyl-phosphate synthetase-aspartate transcarbamoylase-dihydroorotase (CAD)	34	YVAPPSLR	242,829	220,000
		33	SVGEVMGIGR		
		83	MALLATVLGR		
		37	LSLDDLLQR		
		54	TLGVDLVALATR		
		38	AALVLEDGSVLR		
NP_612409.1	Nucleolar MIF4G domain-containing protein 1 (MOM1)	51	SADEANVLR	96,198	105,000
		76	TAGPEQGPGLGGR		
		40	VVEFSELDKPR		
		37	DGLDYILGALESGK		
		68	ALLAANEEEDREIR		
NP_031381.2	Heat shock protein HSP 90-beta isoform a (HSP90AB1)	39	EQVANSAFVER	83,212	80,000
		44	ELISNASDALDK		
		42	TLTLVDTGIGMTK		
		49	GVVDSEDLPLNISR		
		32	HLEINPDHPIVETLR		

NP_004199.1	Apoptosis-inducing factor 1, mitochondrial isoform 1 precursor (AIFM1)	35	ISGLGLTPEQK	66,859	66,000
		47	ALGTEVIQLFPEK		
		34	TGGLEIDSDFGGFR		
		42	VMPNAIVQSVGVSSGK		
		38	VLIVSEDPELPYMRPPLSK		
NP_001393.1	Elongation factor 1-alpha 1 (EEF1A1)	39	IGGIGTVPVGR	50,109	50,000
		39	EHALLAYTLGVK		
NP_116093.1	Tubulin alpha-1C chain (TUBA1C)	35	EIIDLVLDR	49,863	50,000
NP_001530.1	DnaJ homolog subfamily A member 1 (DNAJA1)	64	QISQAYEVLSDAK	44,839	43,000
NP_003312.3	Elongation factor Tu, mitochondrial precursor (TUFM)	44	LLDAVDTYIPVPAR	49,843	43,000
NP_054768.2	Acyl-CoA dehydrogenase family member 9 (ACAD9)	41	ELFLGKIKK	68,717	43,000
NP_001203.1	Complement component 1 Q subcomponent-binding protein, mitochondrial precursor (C1QBP)[b]	92	EVSFQSTGESEWK	31,343	32,000
		58	MSGGWELELNGTEAK		
		37	AFVDFLSDEIKEER		
NP_001143.2	ADP/ATP translocase 2 (SLC25A5)	36	EQGVLSFWR	32,831	32,000

		40	LLLQVQHASK		
		63	DFLAGGVAAAISK		
NP_000998.1	40S ribosomal protein S4, X isoform X isoform (RPS4X)	47	LSNIFVIGK	29,579	32,000
NP_036555.1	60S ribosomal protein L13a isoform 1 (RPL13A)	57	YQAVTATLEEK	23,562	27,000
NP_006004.2	60S ribosomal protein L10 isoform a (RPL10)	46	FNADEFEDMVAEK	24,588	27,000

[a] Highest score is -10*log(P), where P is the probability that the observed match is a random event. A score > 32 indicates identity or extensive homology ($p<0.05$).

[b] Complement component 1 Q subcomponent-binding protein (C1QBP) is also designated mitochondrial matrix protein p32.

Table 2. Effect of the UL47 null-mutation on distribution of virus particles in infected Vero cells.

Virus	% of virus particles in morphogenetic stage[a]					Total counted (particles/cells)
	Nucleocapsids in the nucleus	Enveloped virions in the perinuclear space	Nucleocapsids in the cytoplasm	Enveloped virions in the cytoplasm	Extracellular enveloped virions	
HSV-1 (F)	34.1 (1040)	19.9 (606)	11.0 (336)	13.7 (419)	21.3 (650)	3051/20
YK545(ΔUL47)	63.8 (662)	0.4 (4)	5.3 (56)	3.8 (39)	26.7 (277)	1038/20
YK546(ΔUL47-repair)	38.3 (1102)	15.9 (458)	9.8 (281)	12.3 (356)	23.7 (684)	2881/20

[a] Number in parenthesis is the number of virus particles.

Table 3. Effect of the UL47 null-mutation on distribution of virus particles in infected HEp-2 cells.

Virus	% of virus particles in morphogenetic stage[a]					Total counted (particles/cells)
	Nucleocapsids in the nucleus	Enveloped virions in the perinuclear space	Nucleocapsids in the cytoplasm	Enveloped virions in the cytoplasm	Extracellular enveloped virions	
HSV-1 (F)	26.6 (579)	13.8 (300)	9.7 (211)	19.9 (434)	30.0 (652)	2176/20
YK545(ΔUL47)	61.7 (587)	0.3 (3)	5.8 (55)	4.8 (46)	27.4 (266)	952/20
YK546(ΔUL47-repair)	30.2 (687)	13.1 (298)	9.2 (208)	19.4 (442)	28.1 (638)	2273/20

[a] Number in parenthesis is the number of virus particles.

Table 4. Effect of p32 knock down on distribution of virus particles in infected HEp-2 cells.

Cell type	Number of intra-nuclear invaginations	% of virus particles in morphogenetic stage[a]						Total counted (particles/cells)
		Nucleocapsids in the nucleus	Enveloped virions in the intranuclear invaginations	Enveloped virions in the perinuclear space	Nucleocapsids in the cytoplasm	Enveloped virions in the cytoplasm	Extracellular enveloped virions	
sh-Luc-HEp-2	1	22.3 (639)	0.1 (4)	13.0 (372)	7.9 (228)	23.7 (678)	33.0 (947)	2868/22
sh-p32-HEp-2	21	30.5 (607)	5 (101)	14.8 (295)	13.5 (268)	16.3 (324)	19.9 (396)	1991/22

[a] Number in parenthesis is the number of virus particle

Table 5. Oligonucleotide primers used for construction of the recombinant viruses in this study.

Mutation	Primer	Sequence (5’-3’)
MEF-p32	Forward primer	CGCCGCCGCCGCCAGCTTCCGGTCGAGGTACCTAGGCTAGAACTAGTATGCTGCCTCTGCTGC GCTGCGT
	Reverse primer	GGAATATCATAATCACGCGTCAAGTCCTCTTCAGAAATGAGCTTTTGCTCCTGGCTCTTGACAA AACTCT
MEF-UL34	Forward primer	GAACCCTTTGGTGGGTTTACGCGGGCACGCACGCTCCCATCGCGGGCGCCATGGAGCAAAAG CTCATTTC
	Reverse primer	CCCTCGAAGGCGTCACCTGGGTGGCCGGTGTAGGGCTTGCCCAGTCCCGCATCTTTGTCATCG TCGTCCT
MEF-UL31	Forward primer	CTCGATCTCGCTCCTGTCCCTGGAGCACACCCTGTGTACCTATGTATGACGAGCAAAAGCTCAT TTCTGA
	Reverse primer	TCCTTGCCGTGATAGGGCCCGGGCCGGGAGCCGCGGCGATGGGGGTCGGTATCTTTGTCATCG TCGTCCT
MEF-UL47	Forward primer	TTCTTTTTTGGGGGGTAGCGGACATCCGATAACCCGCGTCTATCGCCACCATGGAGCAAAAGC TCATTTC
	Reverse primer	CGGGGGCGGGTGGATGCGCGCCTCCTACGCCCCGCGGGTTCGCGAGCCGAATCTTTGTCATCG TCGTCCT